Stony Brook University

Tubular localization and cytoskeletal association of over-expressed caveolin-1 in breast cancer cells

A Dissertation Presented

By

Prakhar Verma

To

The Graduate School

In Partial Fulfillment of the

Requirements

For the Degree of

Doctor of Philosophy

In

Biochemistry and Structural Biology

Stony Brook University

May 2009

Stony Brook University

The Graduate School

Prakhar Verma

We, the dissertation committee for the above candidate for the Doctor of Philosophy degree, hereby recommend acceptance of this dissertation.

Deborah A. Brown, Ph.D. – Dissertation Advisor
Professor, Department of Biochemistry and Cell Biology,
Stony Brook University

Neta Dean, Ph.D. – Chairperson of Defense
Professor, Department of Biochemistry and Cell Biology,
Stony Brook University

Robert S. Haltiwanger, Ph.D.
Professor and Interim Chair, Department of Biochemistry and Cell Biology,
Stony Brook University

Aaron M. Neiman, Ph.D.
Associate Professor, Department of Biochemistry and Cell Biology,
Stony Brook University

Nancy C. Reich, Ph.D.
Professor, Department of Molecular Genetics and Microbiology,
Stony Brook University

This dissertation is accepted by the Graduate School

Lawrence Martin
Dean of the Graduate School

Abstract of the Dissertation

Tubular localization and cytoskeletal association of over-expressed caveolin-1 in breast cancer cells

By

Prakhar Verma

Doctor of Philosophy

In

Biochemistry and Structural Biology

Stony Brook University

2009

Caveolin-1 is a major structural component of caveolae, which are small 50 nm plasma membrane invaginations found in different cell types. Expression of caveolin-1 is often lost in breast cancer. The goal of this dissertation is to see whether caveolin-1 localizes abnormally when re-expressed in breast cancer cells, with the long-term goal of understanding how caveolin-1 might act as a tumor suppressor. We found that re-expressing caveolin-1 in breast cancer cells induced formation of long tubules rarely seen in normal cells. Tubule frequency in several transfected lines correlated inversely with endogenous caveolin-1 expression. Tubules were endocytic, required microtubules and membrane cholesterol, and were labeled with EHD proteins and Rab8. Constitutively-active Rab8 and caveolin-1 synergized to promote tubule formation. Caveolin-1 re-expression also induced formation of short plasma membrane-proximal tubules that

associated with actin filaments and required actin but not microtubules. Tubules of both classes were under tension and often snapped, after which ends recoiled. This destabilized tubules, and net tubule length decreased during observation of live cells. Tension was exerted by interactions with actomyosin, as long tubules appeared relaxed, rarely snapped, and were stabilized upon actin filament depolymerization or inhibition of the actomyosin motor myosin II with blebbistatin. These data suggested that the ability of cells to limit caveolin-1-induced membrane tubulation is reduced in luminal breast cancer. Furthermore, we found that actomyosin interactions exert tension on caveolin-1-positive membranes, possibly contributing to caveolin-1 function in directed migration and mechanotransduction in normal cells.

.

Dedication

To

My parents Mahesh and Veena Verma

Table of Contents

Abbreviations

AF	Alexa-Fluor
AMF	Autocrine motility factor
BFA	Brefeldin A
EHD	Eps15 homology domain
ErbB2	Epidermal growth factor receptor 2
CHO	Chinese hamster ovary
CSD	Caveolin scaffolding domain
CT	Cholera toxin
CTxB	Cholera toxin B subunit
DRM	Detergent resistant membranes
EEA1	Early endosomal antigen 1
EGFR	Epidermal growth factor receptor
ER	Endoplasmic reticulum
FYVE	Fab1p-YOPB-Vps27p-EEA1 domain
GPI	Glycosyl phosphatidylinositol
LatA	Latrunculin A
MBCD	Methyl-β-cyclodextrin
PBS	Phosphate buffered saline
PDGF	Platelet-derived growth factor
PH	Pleckstrin homology domain
PLC	Phospholipase C
Rh-Tf	Rhodamine-conjugated Tf
SDS-PAGE	Sodium dodecyl polyacrylamide gel electrophoresis
SV40	Simian virus 40
Tf	Transferrin
Tfr	Transferrin receptor
TRβ	Transforming growth factor receptor β
GalTrans	YFP-galactosyl transferase

List of Figures

List of Tables

Acknowledgements

I would like to start by thanking my graduate advisor, Dr. Deborah A. Brown, for accepting me in the lab as a graduate student. She is a great advisor, always open to questions and scientific discussions. She knows a lot about her subject and works really hard which is really inspiring.

I would like to thank my committee members for asking critical questions, finding problems and suggesting solutions to them. Thanks to all of them for taking time out for proposal defense, committee meetings and dissertation defense.

I would like to thank all of the members of the Brown lab. Anne Ostermeyer-Fay, a research scientist in Brown lab, taught me all the techniques used in the lab. She answered my millions of questions in last five years. I would like to thank former graduate student, Dr. Daniel Barr, for helping me with deconvolution microscopy, with committee meetings and dissertation defense. I am thankful to former postdoctoral fellow Dr. Laura Listenberger for tips and advice. Thanks to Azad Gucwa, a graduate student in Brown lab, for being an awesome friend and for making the daily grind of graduate school fun. Thanks to Catherine Peterson for the cholera toxin and Golgi experiments.

I would like to thank my Good friends Ashish Rai, Prateek Gangwal, and Mayuresh Korgoankar for their friendship and support.

I would like to thank my parents, my sister and my family in India for being understanding, patient and supportive.

Finally, I would like to thank Unnati Shah for being a wonderful person and sharing all the good and bad times in the last four years.

Chapter 1. Introduction

I am going to give a brief introduction of my first project – ErbB2 internalization and trafficking induced by caveolin-1 expression. Later, I will describe my second project in detail. The second project constitutes the bulk of my dissertation.

The project that I proposed initially was based on the data that suggested that caveolin-1 expression trigger internalization in caveolin-1 positive structures. I proposed experiments to follow up this novel observation. The second project also revolves around caveolin-1 and its interaction with cytoskeleton. For this reason, I will describe caveolin-1, caveolar endocytosis and cytoskeleton in detail.

ErbB2 receptor family

ErbB2 (also called as HER2 or Neu), a receptor tyrosine kinase of the EGF receptor family, is overexpressed in 25-30% of human breast cancer, and is associated with poor prognosis (Citri et al., 2002). For this reason, strategies for down-regulation of ErbB2 are of great interest. ErbB2 is transmembrane tyrosine kinase receptors with an extracellular ligand binding domain, a single transmembrane domain and a cytoplasmic kinase domain (Yarden and Sliwkowski, 2001). ErbB2 is unique as it does not have any known ligand (Yarden, 2001). ErbB2 plays an important role in the EGF family by

coordinating with other family members to regulate cellular growth, differentiation and survival. ErbB2 is the most potent oncogenic receptor of all. ErbB2 is over expressed in many cancers especially breast, gastric, lung, and prostate cancers, and is associated with poor prognosis (Roskoski, 2004; Yarden and Sliwkowski, 2001). The down-regulation of ErbB2 can reverse the transformation of cultured cancer cells, and is an important therapeutic target (Klapper et al., 2000).

ErbB2 receptor Internalization

ErbB2 receptor can be internalized and down regulated in at least two ways. One approach is the use of certain monoclonal antibodies directed against ErbB2. One of these antibodies, called herceptin or trastuzumab, is now in use in the clinic. The mechanism of down regulation is not clear, but appears to involve the c-Cbl-dependent pathway, which is also involved in down regulation and degradation of EGFR following ligand binding (Levkowitz et al., 1999; Yarden, 2001).

A second approach to down regulating ErbB2 is to treat the cells with benzoquinone ansamycin antibiotics such as geldanamycin (GA) (Citri et al., 2002; Xu et al., 2001). GA mediates ErbB2 down-regulation by a c-Cbl independent mechanism. Instead, GA inactivates the cellular chaperone Hsp90. Hsp90 binds to its client proteins in their mature form, even after folding is

complete, and keeps them in a stable form (Isaacs et al., 2003). ErbB2 is one the client proteins of Hsp90. GA binds to the nucleotide binding site of the Hsp90 and makes it fall off the receptor. Blocking the Hsp90 ATP binding site favors its dissociation from ErbB2 and promotes the formation of an alternative complex of ErbB2 with Hsp70. A novel E3 ubiquitin ligase called CHIP is recruited to this alternative complex and ubiquitylates ErbB2 (Murata et al., 2003). ErbB2 is then internalized from the plasma membrane by an unknown mechanism and is ultimately degraded. The protein is not targeted to lysosomes as shown by insensitivity to chloroquine. Rather, degradation appears to be proteasome dependent and is blocked by the proteasome inhibitor lactacystin (Xu et al., 2002; Zhou et al., 2003). However, nothing is known about the internalization pathway.

Caveolae and caveolin-1

My second project also dealt with abnormal expression of proteins in breast cancer. The protein caveolin-1, which forms caveolae, is often lost in breast cancer and other cancers. This has suggested that caveolin-1 may act as a tumor suppressor, although the mechanism is not known. The long-term goal of my second project is to determine whether caveolin-1 localization and trafficking play roles in the activity of caveolin-1 as a tumor suppressor. As part of this effort, I found that caveolin-1 formed unusual structures when expressed in breast cancer cells, that were rarely seen in normal cells. These were membrane tubules,

induced by caveolin-1 formation. Characterizing these tubules was a major goal of my project.

As will be discussed below, when caveolin-1 is lost from cells, they also lose structures called caveolae, that depend on caveolin-1. Caveolae are 50-70 nm pits on the plasma membrane of many mammalian cells (Smart *et al.*, 1999). Caveolae are unique flask shaped invaginations easily identified by electron microscopy (Fig. 1).

Figure 1. Electron micrograph showing caveolae (taken from (Shaul and Anderson, 1998)). Fibroblast cells were subjected to rapid-freeze and deep-etch and processed for electron microscopy. Caveolae with variable amounts of curvature are visible on the surface of plasma membrane.

Caveolae are abundant in smooth-muscle cells, fibroblast, adipocytes and endothelial cells but undetectable in cells like lymphocytes and neurons (Parton and Simons, 2007). Caveolin-1 is the mains scaffolding protein of caveolae. Caveolin-1 binds to cholesterol and sphingolipid enriched domains within lipid rafts. Caveolin-1 is a 22 KDa protein with hydrophilic N and C terminal

cytoplasmic domains and a hydrophobic 33-residue middle domain (Schlegel *et al.*, 1999). Caveolin-1 forms homodimers and heterodimers with caveolin-2. Caveolin-1 is absolutely essential for caveolae formation. Caveolin-1 forms heterodimers with caveolin-2 to form higher order oligomers of about 350-400 kDa (Monier *et al.*, 1995). Caveolin-1 is a small protein with an unusual topology. The N- and C-termini of caveolin-1 are cytoplasmic and flank the 33-residue membrane-anchored hydrophobic domain.

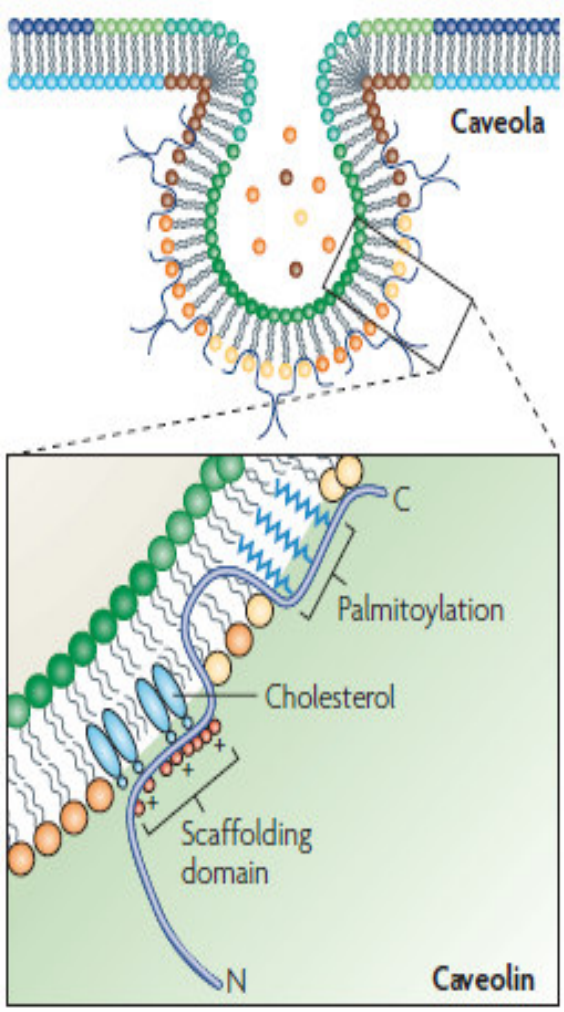

Figure 2. Membrane topology of caveolin-1 (taken from (Parton and Simons, 2007)). The figure shows how caveolin-1 is inserted into caveolar membrane. The hydrophilic N and C termini are cytoplasmic and the hydrophobic region is inserted into the lipid bilayer. The enlarged portion at the bottom shows the caveolin-1 scaffolding domain with conserved basic residues (+) and bulky hydrophobic residues (red dots). The three palmitoyl groups (blue) close to the C terminus are shown inserted in the bilayer.

The region of caveolin-1 responsible for making higher order oligomers spans the sequence from residues 61-103 and is called the oligomerization domain. A 20-residue segment at the end of N-terminal domain (residues 82-101) is called the caveolin scaffolding domain (CSD). The central domain from residues 102-134 is hydrophobic and is inserted in the inner leaflet of the plasma membrane. The C-terminal has three palmitoylation sites at Cys133, -143, and -156 which help caveolin associate with the plasma membrane. CSD is required for caveolin oligomerization and interaction of caveolin with other signaling proteins. CSD can bind to Src family tyrosine kinases, G proteins and G-protein-coupled receptors (GPCRs), endothelial nitric oxide synthase (eNOS) and growth factor receptors (Li *et al.*, 1996; Garcia-Cardena *et al.*, 1997; Ostrom and Insel, 2004). Studies have shown that the CSD is enough to bind and activate Src kinase, GPCRs and that peptides derived from CSD are sufficient to block signaling of Src kinases and GPCRs. This suggests a role for caveolin-1 in the regulation of signaling.

Caveolae are also enriched in a wide variety of signaling molecules (Echarri *et al.*, 2007). Many signaling molecules have been shown to bind directly to caveolin-1. When this occurs, signaling proteins are maintained in an inactive conformation. This has been suggested to partially explain how caveolin-1 might act as a tumor suppressor. Caveolae have been functionally implicated in several other important cellular functions as well - endocytosis, transcytosis, cell polarization and directional migration, and mechanotransduction (Grande-Garcia and del Pozo, 2008). In most cases, it is not understood how caveolae mediate these functions. My work provides a new clue as to how caveolae may function in cell migration and mechanotransduction, which involve the actin cytoskeleton.

Caveolar endocytosis

Endocytosis is very important as it regulates many processes that are aberrant in cancer cells. Several regulators and accessory proteins involved in endocytosis have been shown to behave irregularly in cancer cells (Nichols, 2003). One of the surprising observations I made is that caveolin-1 expressed in breast cancer cells often formed tubules. It is important to understand the trafficking and function of caveolae to understand why caveolin-1 might be forming tubular structures. A brief description of caveolar endocytosis and the role of caveolin-1 as a tumor suppressor protein follow next.

Caveolar endocytosis is the best studied clathrin-independent endocytic pathway (Fig. 3) (Parton and Richards, 2003). Certain pathogens and toxins also take advantage of caveolae to enter the host cells. Several reports have documented the role of caveolae in SV40 virus, cholera toxin (CT) and tetanus toxin endocytosis (Montesano *et al.*, 1982; Parton *et al.*, 1994; Munro *et al.*, 2001; Torgersen *et al.*, 2001). Studies based on fluorescence recovery after photobleaching (FRAP) have shown that caveolae are normally quite stable on the cell surface (Thomsen *et al.*, 2002). At steady state only few caveolae internalize, indicating a slow basal turnover rate (Thomsen *et al.*, 2002; Tagawa *et al.*, 2005). Caveolae can be induced to undergo endocytosis under certain conditions or by binding of certain cargos. The binding of cargo, like SV40 or CT, stimulates caveolar internalization. A study reported that SV40 induces extensive actin tail formation and rearrangement during endocytosis through caveolae (Pelkmans *et al.*, 2002). The other salient features of the pathway include cholesterol dependence, tyrosine kinase dependence and a requirement for dynamin. The autocrine motility factor (AMF), albumin, fluorescent glycosphingolipid (GSL) analogs, and the transforming growth factor-β receptor (TRβ) are the other examples of cargo internalized through caveolae. Caveolar endocytosis is best understood for SV40 virus. Pelkmans *et al.,* showed that the virus enters the cell through caveolae, resides in the novel vesicular structure of neutral pH called caveosomes, and finally reaches the smooth ER by traveling along microtubules

(Pelkmans *et al.*, 2001).

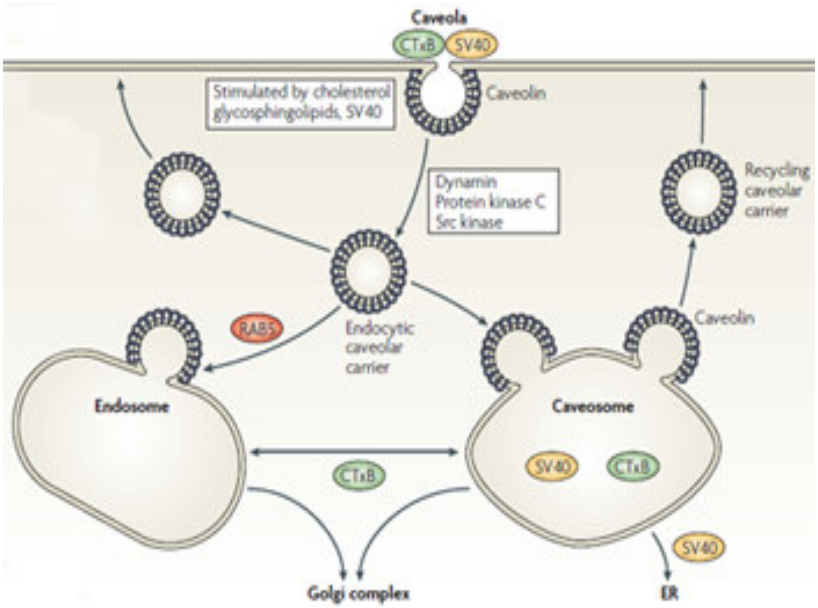

Figure 3. Overview of caveolar endocytosis (taken from (Parton and Simons, 2007)). Caveolar endocytosis is dependent of dynamin, protein kinase C, src kinase and is stimulated by cholesterol and glycosphingolipids. Early endocytic vesicles can either go to caveosomes, endosomes or return back to plasma membrane. Caveosomes are caveolin-1 positive organelles with neutral pH. SV40 is transported to the endoplasmic reticulum (ER) and recycling endocytic caveolar carriers carry caveolin back to the plasma membrane. Cholera toxin is transported to the Golgi complex, possibly through early endosomes.

The ultimate destinations of different cargoes, internalized in caveolae, are different (Fig. 3), which adds to the confusion and complexity of the pathway. SV40 accumulates in smooth ER, while CtxB accumulate in the Golgi (Lencer and Tsai, 2003). Although the pathway is becoming increasingly well characterized by studies involving SV40 as a marker, a physiological role for this pathway has not yet been assigned.

Role of caveolin-1 in cancer

I used human breast cancer cell line, SKBr3, for my studies. Caveolin-1 has a complex relationship with cancer. In many cases, caveolin-1 is lost from tumor cells, suggesting a role as a tumor suppressor. My project has focused on this role. In addition, though, caveolin-1 expression remains high in certain other types of cancer, suggesting a role as an oncogene. It is not understood how caveolin-1 can play these very different roles. Caveolin-1 may have different functions in different cell types, or in different stages of cancer. It is important to understand what is already known about caveolin-1 as a tumor suppressor protein, as will be described next.

Several studies have supported the role of caveolin-1 as a tumor suppressor. Caveolin-1 has been reported to interact directly with signaling molecules, leading to their inactivation (Li *et al.*, 1995). A suggestive piece of evidence came from the fact that caveolin-1 gene is located on human chromosome 7q31.1 which is often deleted in human cancers (Engelman *et al.*, 1998). Also, about 16% of cancers have been reported to have a dominant negative mutation (P132L) in caveolin-1 that disrupts the CSD binding to other proteins (Hayashi *et al.*, 2001). A study by Koleske *et al.,* showed that when NIH 3T3 cells were transformed with several oncogenes, the levels of caveolin-1 were found to be reduced (Koleske *et al.*, 1995). The same group found that caveolin-1 expression in transformed cells was enough to abolish anchorage-independent

growth (Engelman *et al.*, 1997). Another study showed that NIH 3T3 cells can be made to undergo transformation by knocking down caveolin-1 using anti-sense oligos (Galbiati *et al.*, 1998). Caveolin-1 levels are found to be reduced in lung cancer, breast cancer, colon cancer, tumors of ovarian carcinomas, sarcomas and osteosarcomas (Quest *et al.*, 2008). Furthermore, mice with the caveolin-1 gene deleted showed increased susceptibility to epidermal hyperplasia and tumor growth and metastasis (Capozza *et al.*, 2003). The tumor suppressor effect of caveolin-1 could be attributed to its ability to bind to different growth receptors and other effectors of signaling pathways and sequester them in specialized domains in plasma membrane (Goetz *et al.*, 2008).

On the other hand, many studies support the oncogenic role of caveolin-1 or refute the role of caveolin-1 as tumor suppressor. High levels of caveolin-1 are associated with many late stage and metastatic cancer cell lines, multi-drug resistant cell lines, renal cell, esophageal, and squamous cell carcinomas (Kato *et al.*, 2002; Joo *et al.*, 2004; Tsao *et al.*, 2007).

In light of so many contradicting reports, one way to explain the role of caveolin-1 would be to describe caveolin-1 as a restricted or conditional tumor suppressor (Quest *et al.*, 2008). During the initial stages of tumorigenesis, lowering the levels of caveolin-1 helps cancer cells evade the block on growth pathways. However, during tumor progression several changes occur at the molecular level. The tumor suppressing molecules that interact with caveolin-1

are replaced by tumor promoting molecules (Quest *et al.*, 2008). This is evident from the fact that many advanced stage and aggressive cancers have high levels of caveolin-1.

EHD proteins

In this section I am going to describe the Eps15 homology domain (EHD) family proteins. EHD proteins have been reported to make tubular structures in cells which are strikingly similar to the membrane tubules of caveolin-1 we observed in SKBr3 cells. Understanding why EHD proteins make tubules may help us comprehend why caveolin-1 make tubules in SKBr3 cells.

The four members of the Eps15 homology (EH) domain-containing protein family have recently been discovered independently by several groups (Pohl *et al.*, 2000; Iwahashi *et al.*, 2002; Shao *et al.*, 2002a). All mammals have four members in the EHD family, EHD1-4. The four EHD proteins, EHD1-EHD4, have an approximate molecular mass of 60Kda and have three distinct regions – a well-conserved N-terminal loop which includes a nucleotide-binding P-loop motif, a central non-conserved coiled-coil domain, and the third conserved C-terminal EH domain (Mintz *et al.*, 1999; Pohl *et al.*, 2000). The schematic diagram of EHD1 is shown in figure 4.

Figure 4. The domain architecture of EHD1 protein (taken from (Naslavsky *et al.*, 2004a)). The N terminal P-loop, a central coiled coil (CC) and a C terminal EH domain is shown with the numbers indicating the position of amino acids.

Several groups have identified roles for EHD protein in intracellular trafficking, especially in recycling. Numerous studies have shown the role of EHD1 in recycling of MHC-1, the cystic fibrosis transmembrane conductance regulator (CFTR), the glutamate receptor gluR1 and insulin-like growth factor receptor (Grant *et al.*, 2001; Rotem-Yehudar *et al.*, 2001; Caplan *et al.*, 2002; Blume *et al.*, 2007). EHD2 is required for trafficking of insulin-stimulated GLUT4 in adipocytes (Guilherme *et al.*, 2004a; Park *et al.*, 2004). EHD3, like EHD1, has been shown to regulate the traffic between early endosomes and other organelles, especially the Golgi (Naslavsky *et al.*, 2009). EHD4, also known as Pincher, has been shown to regulate the endocytosis and trafficking of nerve growth factor (NGF) and its receptor TrkA in PC12 cells (Shao *et al.*, 2002b).

Tubular localization and interaction of EHD protein family members with other proteins

We found caveolin-1 in tubular structures which look very similar to the tubules formed by the EHD family proteins. The tubules of EHD proteins have been reported to interact with other proteins involved in recycling. This might give clues about function of caveolin-1 tubules.

Because of functional and structural overlap, EHD proteins interact with each other and with other proteins. A study found EHD4 on tubular and vesicular structures when expressed alone and in conjunction with EHD1 and 3. (George *et al.*, 2007). Another study found EHD1 and EHD3 on vesicular and tubular structures involved in Tf recycling (Galperin *et al.*, 2002). Furthermore, C- and N-terminal deletion mutants of EHD3 failed to localize in tubules. A separate report showed that EHD1 and 4 colocalize with each other on microtubule dependent tubular structures (Galperin *et al.*, 2002).

The EHD proteins have been shown to bind to syndapins, a family of proteins involved in linking membrane trafficking and cortical actin cytoskeleton (Braun *et al.*, 2005). A recent study demonstrated the involvement of EHD3 in Rab11-mediated recycling and its interaction with Rab11 through Rab11-FIP2, an effector protein of Rab11 (Naslavsky *et al.*, 2006). Rabenosyn-5, an effector of Rab4/Rab5, binds to EHD1 and regulates the transport of receptor from early endosomes to recycling compartment. The endocytosis of insulin-like growth factor receptor (IGF-1R) is regulated by a complex of EHD1 and SNAP29, a synaptosomal associated protein (Rotem-Yehudar *et al.*, 2001). The recycling of

GLUT4 has been shown to be regulated by EHD1 and EHBP1 (Guilherme *et al.*, 2004b). EHD4/Pincher binds to adaptor protein Numb which is reportedly involved in endosomal recycling and intracellular trafficking of receptors (Smith *et al.*, 2004).

Rab proteins

Like EHD proteins, Rab8 is also known to be localized on tubular structures. Strikingly, in our study we found that caveolin-1 tubules colocalized perfectly with Rab8 tubules. Furthermore, caveolin-1 also enhanced the ability of Rab8 to form tubules. For this reason, I will give a brief introduction to the Rab family and the Rab8 protein.

Rab proteins are molecular switches, and belong to the same super-family as Ras, Rho and Ran. Rabs form the largest monomeric GTPase family. Like their family members, they have a GDP-bound inactive state and a GTP-bound active state. Once activated, the Rab protein can then bind to the effector proteins, (such as early endosomal antigen 1 (EEA1) for Rab5), and promote vesicle fusion. Rab8 has been reported to be mainly involved in membrane transport from trans-Golgi network to plasma membrane (Zerial and McBride, 2001). Rab8 regulates basolateral transport in polarized epithelial kidney cells. Rab8 is also important for maintaining the polarity of a cell (Sato *et al.*, 2007a). A recent report found that Rab8 is essential for the morphogenesis and membrane

trafficking (Hattula *et al.*, 2006). The same study further found that Rab8 localizes to the tubular structures that traffic towards the center of the cell and then recycles back to the plasma membrane.

The cytoskeleton in mammalian cells

A major focus of my project was how caveolin-1 tubules interact with actin and microtubule cytoskeletal elements. This next section gives a brief overview of cytoskeleton and motor proteins in a cell. The caveolin-1 membrane tubules are dependent on actin and microtubules cytoskeleton. As our data suggest, cytoskeleton play an important role in dynamics of caveolin-1 membrane tubules.

Two major types of cytoskeleton in a cell are actin filaments and microtubules (Fuchs and Yang, 1999). Microtubules are mainly involved in vesicular trafficking, organelle and protein movement (Welte, 2004). The actin cytoskeleton is believed to regulate polarity, contractile, motility processes, endocytosis and intracellular trafficking (Sjoblom *et al.*, 2008). Microtubules are polymers of a globular protein, tubulin. Tubulins, the basic structural units of microtubules, polymerize to form linear filaments called protofilaments. Tubulins are of two types – α and β. The head to tail association of α/β subunits forms a protofilament and make microtubules polar (Li and Gundersen, 2008). When α/β tubulins polymerize, the faster polymerizing end is called the plus end and the

opposite end the minus end. In living cells, the minus end of all microtubules are anchored at the microtubules-organizing center (MTOC), or centrosome, near the nucleus and the plus ends fan out in the cytoplasm towards the plasma membrane (Fig. 5) (Li and Gundersen, 2008).

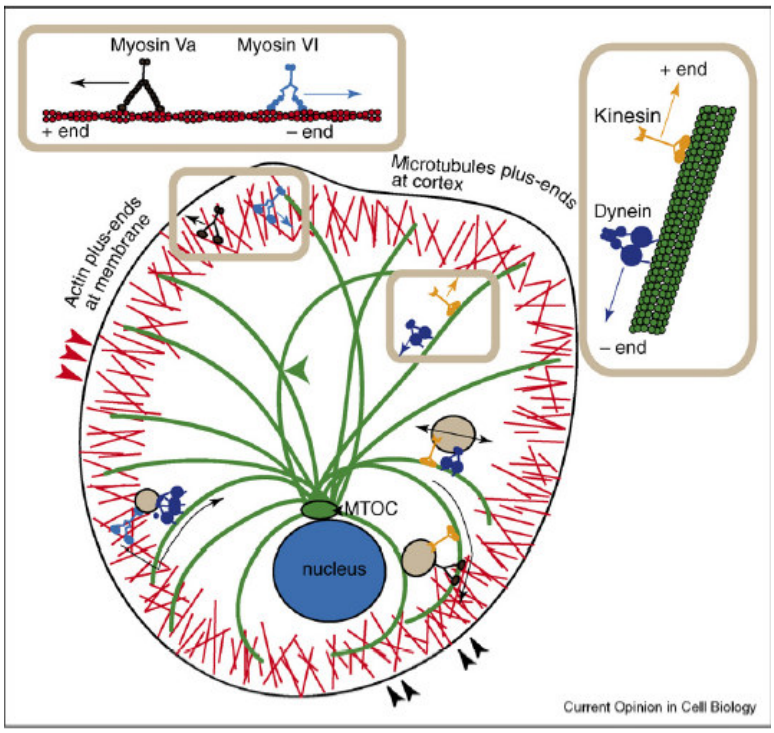

Figure 5. The cytoskeleton network and motor proteins in a cell (taken from (Ross *et al.*, 2008)). Myosin family motors, myosin Va (dark brown) and myosin VI (light blue), walk along actin filaments (red) at the cortex. Myosin Va walks toward the F-actin plus end, which is oriented toward the membrane. Myosin VI walks toward the minus end of F-actin, toward the cell interior. Microtubule-based motors include the kinesin family motors (orange) and cytoplasmic dynein (violet). Kinesin motors walk to the plus ends of microtubules (green), which are oriented toward the actin cortex. Dynein motors walk toward the minus end of the microtubule, which is located at the microtubule-organizing center (MTOC, green) near the cell nucleus (blue). F-actin and microtubules cross at the cell cortex, as highlighted by black arrowheads (lower right). F-actin cross in the cortex, highlighted by the red arrowheads (left). Microtubules can intersect other microtubules highlighted by the green arrowhead (center). Vesicular cargo (tan) can bind to myosin VI and dynein to switch from actin-based to microtubule-based motion while being transported into the cell interior (lower left). Vesicles can bind kinesin and myosin Va to switch from microtubule-based to actin-based motion in order to be transported to the cell cortex (lower right). Vesicles traveling on microtubules can experience a tug of war from kinesin and dynein simultaneously bound (right).

Like microtubules, actin filaments are also dynamic polar polymers of globular actin (G-actin) subunits (Brown, 1999). G-actin subunits polymerize in the same head-to-tail fashion as tubulins to form long filaments called F-actin. F-actin filaments are double helical polymers that have polarity (Pollard and Borisy, 2003). The growing end or the plus end is called the barbed end and the end opposite to it is the pointed end. The barbed end is directed outward towards the membrane (Fig. 5) (Small *et al.*, 1978).

Molecular motors

Our data supports the role of the myosin II motor protein in caveolin-1 membrane tubule extension and contraction. Other molecular motors might be involved in the tubular dynamics with myosin II. For this reason the following section gives a brief overview of different types of motors with emphasis on myosin II.

Molecular motors are the trucks running on cytoskeletal highways. Their function is to bind organelles, vesicles and other cargoes and transport them from one point to another in the cell. There are three different families of molecular motors: dyenins, kinesins and myosins. Myosins regulate transport on actin filaments, and kinesins and dyenins run on microtubules. Most kinesin motors move towards the plus end of microtubules, while dyenin motors carry cargo towards the minus end (Fig. 5) (Endow, 2003; Mallik and Gross, 2004).

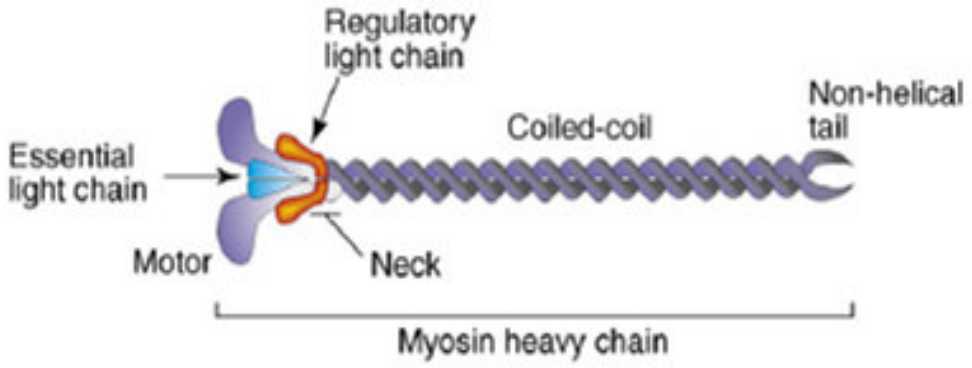

Figure 6. Domain structure of myosin II motor protein (taken from (Clark *et al.*, 2007)). Myosin II monomer has is a hexameric protein with two heavy chains, light chains and regulatory chains. Motor, neck and tail domains are shown.

Every motor protein has a globular motor domain that binds and hydrolyzes ATP and several other regulatory structural domains which assist in oligomerization, cargo binding and movement (Fig. 6). The head domain of motors binds to the filament and use energy of ATP hydrolysis to move along the filament. The tails of some non-muscle myosin motors binds to cargo and can move it along the filaments.

Myosins form a large superfamily of proteins (Hodge and Cope, 2000). It is a two-headed myosin first found in muscle. Myosin II motors are further grouped into different sub-classes based on the sequence of the head domain. Mammals have three different isoforms of non-muscle myosin II – IIA, IIB and IIC, which share a high degree of amino acid sequence similarity (Golomb *et al.*, 2004). The three isoforms have overlapping functions in a cell, but there is increasing evidence that each isoform has a unique role. The isoforms are reported to have an asymmetric distribution in an individual cell (Kolega, 2006), different modes of regulation (Sandquist *et al.*, 2006) and different biochemical properties (Krendel and Mooseker, 2005). Some of the well-studied functions of myosin II are in cytokinesis, where myosin II helps daughter cells to pinch off and move apart from each other (Bao *et al.*, 2005) and in leukocyte movement, where myosin II creates cortical contraction at the trailing edge (Devreotes and Janetopoulos, 2003).

Myosin II, unlike some other myosins, does not bind cargo via a tail domain (Clark *et al.*, 2007). Instead, coiled-coil regions of different myosin II molecules oligomerize in a head-to-tail manner. By this mechanism, myosin II molecules assemble into bipolar filaments. Each filament is capable of interacting with more than one actin filament at the same time. As oppositely-oriented motors try to walk in opposite directions on different actin filaments, the result is induction of tension in the actin network. The cortical actin cytoskeleton under the plasma membrane of mammalian cells forms actomyosin that is under tension by this mechanism.

Chapter 2. Materials and methods

Materials

Cells and transfection

Human breast cancer cell lines, SK-Br-3, MDA-MB-231, MDA-MB-435, NIH 3T3 and COS cells were obtained from American Type Culture Collection (ATCC, Manassas, VA), and were cultured in Dulbecco's modified Eagle's medium with 10% iron-supplemented calf serum (JRH, Lenexa, KS) and penicillin/streptomycin. Cells were transiently transfected with Lipofectamine 2000 or LTX (Invitrogen, Carlsbad, CA) according to the manufacturer's recommendation, and examined 1-2 days post-transfection. Cells transfected with Arf6-Q67L were examined 14-16 hours post-transfection.

Plasmids

Plasmids encoding HA- and myc-tagged canine caveolin-1 have been described (Dietzen *et al.*, 1995). A plasmid encoding the GFP-tagged caveolin-1 was the gift of Douglas Lublin (Washington University School of Medicine, St. Louis). EHD1, EHD2 and EHD3 were provided by Steve Caplan at University of Nebraska Medical Center, Omaha (Caplan *et al.*, 2002; Naslavsky *et al.*, 2004a). EHD4 (Pincher) was the gift of Simon Halegoua, Department of Neurobiology

and Behavior, Stony Brook University (Shao *et al.*, 2002b). HA-tagged constitutively-active Arf6-Q67L (Hernández-Deviez *et al.*, 2004) in pCB7 (Frank *et al.*, 1998) was the gift of J. Casanova (University of Virginia, Charlottesville, VA). pEGFP-Rab8 plasmids (Hattula *et al.*, 2006) were the gift of Johan Peranen (Institute of Biotechnology, University of Helsinki, Finland). GFP-tagged Myosin V plasmids were provided by John A. Mercer (McLaughlin Research Institute, Montana) (Provance *et al.*, 2008). The HA-tagged RhoA plasmids were obtained from the cDNA Resource Center, University of Missouri-Rolla. The Ds-red-Actin plasmid was obtained from Mario J. Rebecchi, Stony Brook University. Human ErbB2 in pcDNA3 was from Len Neckers (NIH).

Antibodies, fluorescent compounds, and other reagents

Anti-ErbB2 antibodies: for immunofluorescence microscopy (IF), monoclonal antibodies 4D5 (purified from supernatant of hybridoma cells (ATCC) grown in an Integra Biosciences CELLine two-compartment bioreactor, from Microbiology International (Frederick, MD)), or 9G6.10 or N28 from LabVision (Fremont, CA) were used for cell-surface detection. Rabbit polyclonal anti-ErbB2 antibodies (DakoCytomation USA, Carpinteria, CA) or the monoclonal antibodies listed above (as indicated) were used on fixed/permeabilized cells. We constructed fluoresceinated anti-ErbB2 Fab

fragments (Fl-Fabs) from N28. Rabbit anti-HA tag antibodies were from Sigma Aldrich (St. Louis, MO). Mouse anti-HSP90 antibody was from Santa Cruz Biotechnology (Santa Cruz, CA). Mouse anti-Myc tag antibody was purchased from Invitrogen (Carlsbad, CA). Rabbit anti-caveolin-1, mouse γ-adaptin, mouse anti-EEA1 and anti-GM130 antibodies were from Transduction Laboratories, BD Biosciences (San Jose, CA). Sheep anti-TGN46 antibody was purchased from AbD Serotec (Raleigh, NC). Rhodamine was conjugated to human Tf using N-hydroxysuccinimide-rhodamine, by the protocol recommended by the supplier. Alexa Fluor (AF)-594-Tf and AF-594-Phalloidin was from Molecular Probes, Invitrogen (Carlsbad, CA). Secondary antibodies; dichlorotriazinylaminofluorescein-goat anti-mouse IgG, fluorescein-goat anti-rabbit IgG, Texas red-goat anti-mouse IgG, Texas red-goat anti-rabbit IgG, horseradish peroxidase-goat anti-mouse and anti-rabbit IgG were from Jackson Immunoresearch Laboratories (West Grove, PA). AF-594-donkey anti-sheep, AF-594-cholera toxin B subunit (AF-594-CTxB) and FluoroRuby^{TM} dextran (10,000 MW) were from Molecular Probes, Invitrogen. Other reagents: Human Tf, Blebbistatin, Brefeldin A (BFA), MBCD and Nocodazole were from Sigma Aldrich (St. Louis, MO). Latrunculin A (LatA) was from Enzo Life Sciences International, Inc. (Plymouth Meeting, PA).

Methods

Fluorescence microscopy

Cells were seeded on glass coverslips in a 35 mm dishes, transfected within 12 to 36 hours if required. After 1-2 days of transfection, cells were treated with drug wherever required and then fixed in phosphate-buffered saline (PBS; 150 mM NaCl, 20 mM phosphate buffer, pH 7.4) containing 3% paraformaldehyde for 30 minutes, permeabilized at room temperature with PBS containing 0.5% Triton and blocked with PBS containing 3% BSA and 10 mM glycine. The primary and secondary antibodies were diluted in 3% BSA and 10 mM glycine. Cells were incubated with primary antibodies for 1 hour at room temperature, followed by secondary antibodies for 30 minutes, also at room temperature. The cells were photographed and images were captured and processed by epifluorescence microscopy as described (Ostermeyer *et al.*, 2001; Ostermeyer *et al.*, 2004) or by deconvolution microscopy using a Zeiss Axiovert 200 deconvolution microscope and processing images with Axiovision software (version 4.7.1). Z- stacks were taken and then deconvolved as described earlier (Barr *et al.*, 2008). All images were acquired with 100x oil immersion objective.

The CtxB and Tf uptake experiments were performed by adding AF-594-CtxB or fluorescent Tf (35 µg/ml) to the regular growth medium and incubating cells in it for times indicated in figure legend. For internalization times greater

than 5 minutes, cells were returned to a 37°C incubator. For internalization times less than 5 minutes, cells were then transferred to a 37°C water bath. Nocodazole (10 µm), LatA (5 µm) and MBCD (10 mM) were dissolved in the pre-warmed media. The cells were exposed to drugs for a specified time, mentioned in figure legend, before processing for fluorescence microscopy.

Time-lapse microscopy

Live cell microscopy was performed on Zeiss Axiovert 200 deconvolution microscope equipped with an Axiocam digital camera (Carl Zeiss, Germany). SKBr3 cells were seeded on 35mm glass bottomed dishes from MatTek Corporation, Ashland, Massachusetts. Cells were transfected as described above and were imaged live after 1-2 days. All images were acquired using 100x oil immersion objective. Images were taken at the frame interval of 10-20 seconds with the exposure time calculated by computer. The images were processed using Axiovision software, release 4.7.1, August 2008.

Tubule measurement

Tubules of caveolin-1-GFP were measured in SKBr3 cells imaged as described above. To compute the net change in the tubule length, two frames, one

at the beginning and one at the end of the stack, were selected. The total length of all the tubules in each frame was measured using Axiovision software. The net change was then calculated by subtracting the total length of tubules at the end from the total length of tubules at the beginning.

Blue native gel electrophoresis

Cells were lysed in lysis buffer (500 mM 6-amino caproic acid, 2 mM EDTA, and 25 mM Bistris, pH 7.0) containing 120 mM *N*-octyl-β-D-glucopyranoside for 30 min at 4°C. Lysates were clarified by centrifugation for 10 min at top speed in a microfuge. Supernatants were mixed with 1/10 volume sample buffer (5% Serva Blue G, 500 mM ε-amino *n*-caproic acid, and 100 mM Bistris, pH 7.0) and 1/10 volume glycerol. Proteins were separated on linear 5.5–16% acrylamide gradient gels run at 100 V at 4°C until the dye reached the middle of the gel. Blue cathode buffer (50 mM Tricine, 15 mM Bistris, and 0.02% Serva Blue G, pH 7.0) was then replaced by colorless cathode buffer (lacking Serva Blue G), and gels were run at 200 V until the dye reached the bottom. After soaking gels for 10 min at room temperature in transfer buffer containing 0.1% SDS, proteins were transferred to PVDF membranes and detected by Western blotting. Sizes were roughly estimated by comparison to standards: apoferritin

(440 kDa), β-amylase (200 kDa), bovine serum albumin (66 kDa), and carbonic anhydrase (29 kDa).

Other methods

Sodium dodecyl sulfate polyacrylamide gel electrophoresis (SDS-PAGE), transfer to polyvinylidene difluoride, Western blotting, and detection by enhanced chemiluminescence were performed as described (Schroeder *et al.*, 1998).

Chapter 3. Results I

This chapter describes the results of my first project – ErbB2 internalization and trafficking induced by caveolin-1 expression. The results are followed by the figures for this part.

ErbB2 internalization is triggered by geldanamycin (GA)

ErbB2 was expressed at high levels on the surface of SKBr3 cells (Fig. 7A), as reported previously (Austin *et al.*, 2004; Hommelgaard *et al.*, 2004). Also as reported (Austin *et al.*, 2004; Hommelgaard *et al.*, 2004), fluorescein-conjugated surface-bound anti-ErbB2 antibodies (Fl-anti-ErbB2) did not greatly affect ErbB2 localization after 2-3 hours of warming (Figure 7B). After 2-3 hours of GA treatment, surface staining was greatly reduced and most of the protein localized to intracellular puncta (Fig. 7C). As previously reported (Austin *et al.*, 2004; Hommelgaard *et al.*, 2004), internalized ErbB2 was first easily visible 30-45 minutes after GA treatment. ErbB2 in GA-treated cells visualized by indirect immunofluorescence had a similar punctate localization, except that somewhat more ErbB2 remained on the cell surface. We next repeated this experiment in COS cells transiently expressing ErbB2. [COS cells endogenously express low levels of ErbB2, detectable in our hands by Western blotting but not by immunofluorescence, (not shown)]. As in SKBr3 cells, Fl-Fabs were efficiently internalized into puncta in GA-treated cells (Fig. 8B). In contrast to their

behavior in SKBr3 cells, however, Fl-Fabs bound to the surface of ErbB2-transfected COS cells were constitutively internalized, even in the absence of GA (Fig. 8A). COS cells express moderate levels of the caveolar coat protein caveolin-1, while SKBr3 cells completely lack caveolin-1 expression, and contain no caveolae. Internalized Fl-Fabs often colocalized with caveolin-1 in COS cells, both with and without GA treatment (not shown). This suggested that Fl-Fab-bound ErbB2 was internalized in caveolae.

Caveolin-1 induces ErbB2 internalization

To test if caveolin-1 induces ErbB2 internalization, we expressed caveolin-1 in SKBr3 cells. As predicted, Fl-Fab bound to cell-surface ErbB2 on caveolin-1 expressing cells was internalized, while Fl-Fab bound to untransfected cells on the same slide remained on the cell surface (Fig. 9). Caveolin-1 induced ErbB2 internalization even without GA treatment (Fig. 9). When overexpressed in COS cells, ErbB2 was also constitutively internalized in association with endogenous caveolin-1, and was localized predominantly in endocytic structures at steady state, both with and without GA treatment (not shown).

ErbB2 is transported to early endosomes

We next examined downstream trafficking of ErbB2 in GA-treated cells expressing caveolin-1. Dan Barr in our lab showed that in GA-treated cells,

ErbB2 internalized for 5 min is in distinctive structures that do not contain co-internalized transferrin (Tf), a marker for clathrin endocytosis. Although ErbB2 showed little co-localization with markers of the clathrin pathway after short internalization times in GA-treated cells (not shown), it colocalized significantly with AF-594-Tf after longer times (Fig. 10A). This suggested that the ErbB2 transport pathway merged with the classical endocytic pathway following internalization. Consistent with this idea, after 2 hours GA treatment, ErbB2 colocalized with the early endosome markers EEA1 (Fig. 10B). ErbB2 was sometimes detected inside structures surrounded with EEA1 in an irregular form (Fig. 10B).

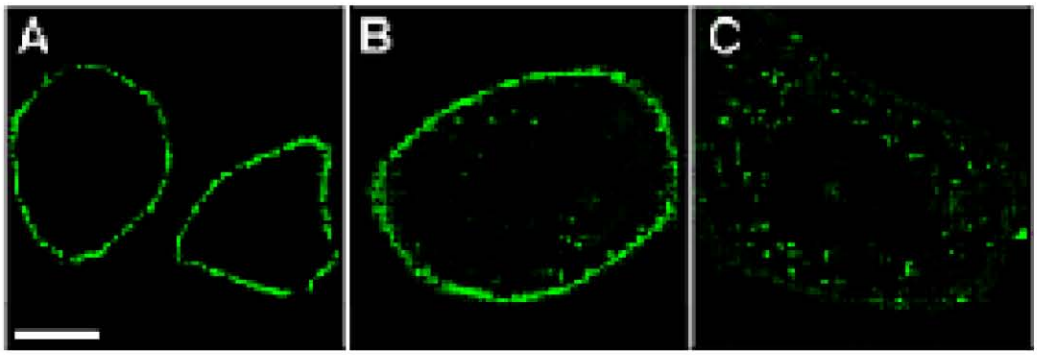
A
B
C

Figure 7. Effect of bound antibodies, geldanamycin on ErbB2 localization in SKBr3 cells. (A) ErbB2 was detected in fixed, permeabilized cells by indirect IF. (B) Cells were warmed for 2 hours after binding Fl-anti-ErbB2 before fixation. (C) Cells were treated with geldanamycin (GA) for 2 hours before fixation, permeabilization, and detection of ErbB2 by indirect IF. Scale bar (applies to all panels); 10 μm.

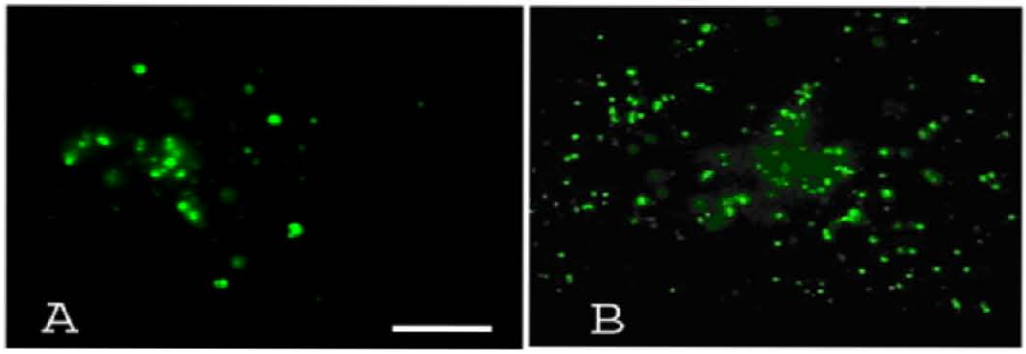
A
B

Figure 8. Effect of bound antibodies, geldanamycin on ErbB2 localization in COS cells. COS cells were transiently transfected with ErbB2, prebound with anti-ErbB2 FI-Fabs, incubated 2 hours in absence (A) or presence (B) of geldanamycin. Scale bar; 10 μm.

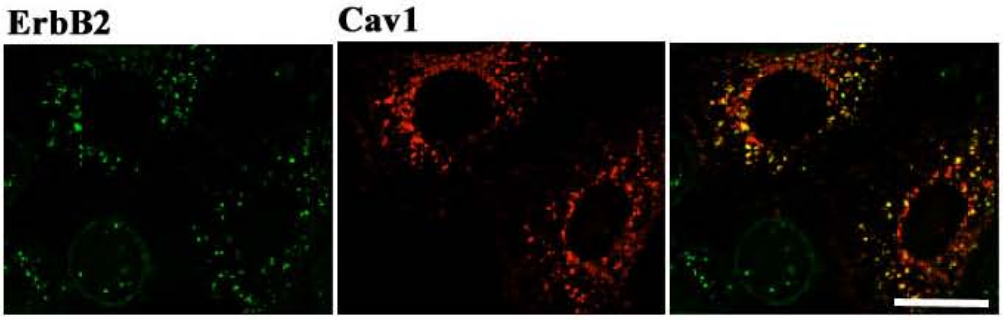
ErbB2
Cav1

Figure 9. ErbB2 colocalize with exogenously expressed caveolin1 in SKBr3 cells. SKBr3 cells were transiently transfected with caveolin-1 and prebound with anti-ErbB2 FI-Fabs, incubated 2 hours before fixing and processing for indirect immunofluorescence. Caveolin-1 was detected by polyclonal anti-caveolin-1 antibody. Scale bar; 10 μm.

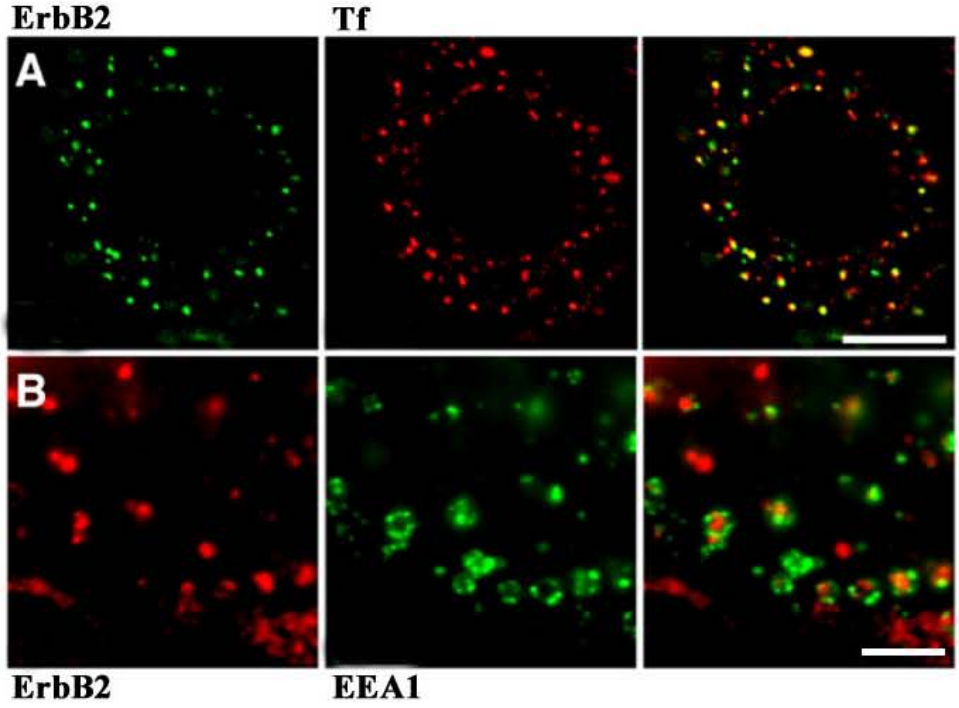
ErbB2
Tf
A
B
ErbB2
EEA1

Figure 10. ErbB2 is delivered to early endosomes after GA treatment in SKBr3 cells. SKBr3 cells were treated with geldanamycin for 2 hours (in media containing Rh-Tf in A), fixed, and permeabilized. (A-B) Left panels; ErbB2, detected with polyclonal antibodies. Center panels: (A) Rh-Tf fluorescence; (B) endogenous EEA1. Right panels; merged images. (A) deconvolved image from a Z stack; (B-D) epifluorescence images. Scale bars; A, 10 μm; B 5 μm

Chapter 4. Results II

While studying the effect of caveolin-1 on ErbB2 internalization in SKBr3 cells, we found caveolin-1 in tubular structures. The tubular localization and cytoskeleton association became my second project and the results are described below.

Localization of caveolin-1 expressed in SKBr3 breast cancer cells.

Caveolin-1 folds and oligomerizes in the ER, and oligomers enlarge further as the protein passes through the Golgi (Scheiffele *et al.*, 1998). We determined whether caveolin-1 oligomerizes normally when expressed in SKBr3 cells, using blue native gel electrophoresis as described earlier (Ren *et al.*, 2004). Caveolin-1 migrated at the position of the normal oligomer when expressed in either SKBr3, Hela, MDA MB-435, or COS7 cells (Fig. 11A). For comparison, migration on blue native gels of wild-type caveolin-1 or a caveolin-1 mutant (Caveolin-102A5, in which 5 residues in the hydrophobic domain are changed to Ala) that does not fully oligomerize, both expressed in COS-7 cells, is shown (Fig. 11B) (Ren *et al.*, 2004). Some mutant Caveolin-102A5 migrates at the monomer position, though the monomer migrates somewhat anomalously because of bound detergent.

In normal cells, caveolin-1 is localized to caveolae, caveosomes, and small vesicles that move between the plasma membrane and the cell interior in a microtubule-dependent manner (Pelkmans *et al.*, 2001; Mundy *et al.*, 2002). Small pools are present in early endosomes (Pelkmans *et al.*, 2001) and in the Golgi in some cell types (Denker *et al.*, 1996; Ren *et al.*, 2004). To determine how this localization pattern might be altered in transformed cells that have lost endogenous caveolin-1 expression, we expressed caveolin-1 in SKBr3 cells. To facilitate live-cell imaging, many of these experiments were done with caveolin-1-GFP or caveolin-1-RFP. Both proteins have been show to localize in the same manner as endogenous caveolin-1 in normal cells (Pelkmans *et al.*, 2001; Mundy *et al.*, 2002), and both showed identical localization patterns in SKBr3 cells.

Caveolin-1-GFP was present in small puncta on and near the plasma membrane, in larger puncta throughout the cytosol, and sometimes in amorphous perinuclear structures (Fig. 12A). The protein was easily detectable in EEA1-positive early endosomes. As in other cells (Pelkmans *et al.*, 2004), co-expression of caveolin-1-RFP with constitutively-active GFP-Rab5 increased the amount of caveolin-1-RFP in endosomes (Fig. 12B). High Rab5 function may slow exit of caveolin-1 from early endosomes, allowing it to accumulate there.

Caveolin-1-positive structures are endocytic

To determine whether the caveolin-1-positive puncta were endocytic, we determined whether they could be labeled with CTxB, which binds cell-surface GM1 and is constitutively internalized by a variety of endocytic pathways (Fig. 13A). After 2 min of internalization, most caveolin-1-GFP-positive puncta close to the plasma membrane were labeled with CTxB. Caveolin-1-positive structures deeper in the cell became labeled with progressively longer internalization times. By 10 min, most peripheral caveolin-1-positive structures (but not the perinuclear structures) were labeled with internalized CTxB, showing that they were endocytic (Fig. 13B). By 60 min of internalization, the perinuclear structures were labeled as well, and the two markers showed good colocalization in them (Fig. 13C).

To determine the nature of these structures, we examined colocalization of various markers with either CTxB or perinuclear caveolin-1-GFP. As expected, CTxB colocalized well with transferrin in early endosomes after 20 min internalization (Fig. 13D). By 60 min, both markers became concentrated in the perinuclear region (Fig. 13E). Although some colocalization in this area was apparent, some CTxB segregated into structures that were not labeled with Tf, showing that they were distinct from the endocytic recycling compartment. As CTxB is known to be transported from endosomes to the Golgi apparatus, we searched for colocalization with Golgi markers. Although CTxB was often close to structures containing the cis-Golgi network (CGN) marker GM130, it did not

colocalize precisely with them (Fig. 14A). The same was true for the cisternal Golgi marker YFP-galactosyl transferase (GalTrans) (Fig. 14B). Treatment with nocodazole to disrupt microtubules slightly enhanced the distinction between the two structures (Fig. 14C). The Golgi is relatively dispersed in SKBr3 cells, and the cisternal Golgi can be distinguished from λ adaptin, a TGN marker (Fig. 14D). CTxB colocalized more closely with the trans-Golgi network marker TGN46 than with YFP-GalTrans, though colocalization was not complete (Fig. 15A).

Additional experiments further probed the relationship of these compartments. Unlike the cisternal Golgi, the TGN does not return to the ER in cells treated with brefeldin A (BFA), but forms stable tubules (Lippincott-Schwartz *et al.*, 1991; Wood *et al.*, 1991). Early endosomes also form tubules after BFA treatment, and markers of the TGN and early endosomes may colocalize on the tubules. After 60 min of CTxB internalization and BFA treatment, the cisternal Golgi marker YFP-GalTrans was largely dispersed to an ER-like staining pattern, as expected (not shown). By contrast, both TGN46 and CTxB were present in membrane tubules in most cells (Fig. 15B). However, tubules labeled by the two markers were almost entirely distinct from each other (Fig. 15B). This suggested that without drug treatment, the perinuclear compartment labeled by CTxB was either distinct from the TGN, or was a different TGN sub-compartment from that containing TGN46.

As seen for CTxB, perinuclear caveolin-1-GFP did not colocalize with GM130 (Fig. 16A) or the cisternal Golgi marker YFP-GalTrans (not shown). It colocalized more closely with TGN46, although colocalization was often incomplete (Fig. 16B). Caveolin-1-GFP was present on tubules in some cells after BFA treatment, but these were distinct from TGN46-positive tubules (Fig. 16C).

It is not known how internalized caveolin-1 recycles to the plasma membrane. We considered the possibility that the perinuclear pool of caveolin-1 might be a recycling compartment. Myosin Vb is required for recycling of cargo internalized by clathrin-dependent and at least some clathrin-independent endocytic pathways. A myosin Vb tail fragment inhibits recycling in a dominant-negative manner, and cargo accumulates in perinuclear structures together with the tail fragment (Lapierre *et al.*, 2001; Roland *et al.*, 2007b). GFP-myosin Vb tail and caveolin-1-RFP colocalized extensively in perinuclear puncta in co-transfected SKBr3 cells, and caveolin-1-RFP was sometimes almost entirely trapped in these structures (Fig. 17A). By contrast, CTxB internalized for 60 min did not colocalize with GFP-myosin Vb tail, but was present in separate perinuclear structures (Fig. 17B). This suggested that caveolin-1-GFP normally recycled via a myosin Vb-dependent pathway, and that inhibition of this pathway by GFP-myosin Vb tail induced segregation of the perinuclear pools of CTxB and caveolin-1.

Caveolin-1-GFP is present in membrane tubules in SKBr3 cells

In addition to the structures described above, caveolin-1-GFP was sometimes present in membrane tubules in SKBr3 cells. These tubules fell into two classes, which we termed long and short. Short tubules had an average length of 2.3 µm ± 0.7. The Short tubules were always connected to the plasma membrane and were restricted to the zone where cortical actin cytoskeleton is located. Long tubules, on other hand, showed great variability in length ranging from 2.5 µm in the center of the cell to 38 µm running across the cell. Most long tubules were connected to plasma membrane. But some appeared severed from the plasma membrane. We do not know if they are actually severed or go out of the focal plane. Long tubules are described next, while short tubules will be described later.

Caveolin-1-GFP-positive long tubules are more common in cancer cells that have lost endogenous caveolin-1 expression

Caveolin-1-positive long tubules (Fig. 18A) were tens of microns long, and often extended deep into the cell. Such tubules have been reported previously in A431 human epithelial carcinoma cells and Chinese hamster ovary (CHO) cells (Parton *et al.*, 1994; Mundy *et al.*, 2002; Peters *et al.*, 2003), but this localization is rare. In SKBr3 cells, caveolin-1-GFP was present in long tubules in 10-20% of transfected SKBr3 cells. To determine whether this localization was unusually

common in these cells, we expressed the protein in several other cell lines. Strikingly, the propensity of caveolin-1-GFP to localize to membrane tubules correlated inversely with the level of endogenous caveolin-1 expression (Fig. 19). When re-expressed in other breast cancer lines that had very low levels of endogenous caveolin-1, or in 435 melanoma cells, caveolin-1-GFP localized in tubules at about the same frequency as in SKBr3 cells. By contrast, in untransformed cells and in breast cancer cell lines that expressed higher levels of endogenous caveolin-1, tubular localization of caveolin-1-GFP was less common. About 1% of untransformed cells or cancer cells with endogenous caveolin-1 had caveolin-1-GFP or endogenous caveolin-1 in tubular structures. This suggested that when cancer cells lose caveolin-1 expression, they also lose the ability to limit caveolin-1-induced membrane tubulation.

The scarcity of caveolin-1 positive tubules has previously made these structures difficult to study. Because the tubules were relatively abundant in SKBr3 cells, we were able to examine them in more detail.

Caveolin-1-GFP tubules were not induced by the GFP tag

The standard way to study the trafficking of a protein in live cells is to attach a fluorescent tag to the protein and follow its movement in the cell. Caveolin-1-GFP and caveolin-1-RFP have been extensively characterized and shown to behave in the same way as endogenous caveolin-1 (Pelkmans et al.,

2001). To rule out the possibility that tubules were an artifact of the GFP tag, we expressed untagged caveolin-1 in SKBr3 cells and compared its localization to that of caveolin-1-GFP. Like caveolin-1-GFP, untagged caveolin-1 localized to membrane tubules (Fig. 20). 10 to 15% cells expressing untagged caveolin-1 showed tubular localization as compared to 15 to 20% of cells expressing caveolin-1-GFP. As these numbers are quite close, caveolin-1-GFP tubules are not the artifact of GFP tag expression.

Caveolin-1 enhances formation of endocytic long tubules

To determine whether the tubules were endocytic, we determined whether they could be labeled with CTxB. Although the tubules were rarely labeled after 2 min of CTxB uptake (not shown), they almost all contained internalized CTxB after 10 minutes, showing that most were endocytic (Fig. 18B). Furthermore, the fact that most tubules could be labeled by CTxB in 10 min showed that they remained closely associated with the plasma membrane. Tubules may have remained open to the plasma membrane, allowing CTxB to diffuse in. Any tubules that detached from the plasma membrane, becoming inaccessible to CTxB, must have been unstable, disappearing within a few minutes. CTxB was very rarely (<1% of cells) seen in long tubules in untransfected SKBr3 cells, and these were never abundant. Thus, caveolin-1-GFP enhanced formation of plasma membrane-derived membrane tubules in SKBr3 cells.

Caveolin-1-GFP long tubules retain plasma membrane characteristics and do not merge with early endosomes

$PI(4,5)P_2$ is abundant in the plasma membrane, but is normally cleaved by phosphatases soon after internalization (Cremona *et al.*, 1999), and is not present at high levels in early endosomes or other organelles. Caveolin-1-positive tubules, even those deep in the cell, could be labeled with the $PI(4,5)P_2$ probe GFP-PH-PLC-delta, showing that they retained this plasma membrane marker (Fig. 18H).

Soon after internalization, vesicles internalized by clathrin-mediated endocytosis and also by several clathrin-independent pathways are delivered to Rab5/EEA1-positive early endosomes, merging cargo internalized by clathrin-dependent and clathrin-independent pathways (Naslavsky *et al.*, 2003; Sharma *et al.*, 2003; Kalia *et al.*, 2006; Barr *et al.*, 2008). By contrast, caveolin-1-RFP tubules did not label for EEA1, or the early endosome-specific phosphoinositide PI(3)P, and did not contain internalized transferrin (Fig. 18D, E and G). Furthermore, we did not see contact between caveolin-1 tubules and EEA1-positive endosomes. Thus, caveolin-1-GFP tubules do not acquire characteristics of early endosomes.

Caveolin-1 tubules are cholesterol dependent

Cholesterol depletion or sequestration induces dramatic flattening of caveolae within a few minutes (Rothberg *et al.*, 1992; Hailstones *et al.*, 1998). To determine the effect of cholesterol on caveolin-1-GFP dynamics and tubule formation in SKBr3 cells, we depleted cholesterol with MBCD. Caveolin-1 long tubules were not seen in MBCD-treated cells (Fig. 21A). Furthermore, small caveolin-1-positive puncta also disappeared after MBCD treatment (Fig. 21A), and caveolin-1-GFP had a smooth appearance in the plasma membrane (Fig. 21A).

SKBr3 cells sometimes exhibit large vacuoles derived from the plasma membrane (our unpublished results). These are likely to be macropinosomes, formed by constitutive plasma membrane ruffling that occurs in these cells. Caveolin-1-GFP-positive vacuoles were especially prominent in MBCD-treated cells, and were seen in most drug-treated cells (Fig. 21A). At least some vacuoles could be labeled with fluorescent dextran, added to media as a marker of fluid phase endocytosis, after 5 min (Fig. 21A). This occurred despite the fact that constitutive internalization of dextran in small endocytic puncta was greatly inhibited by MBCD (not shown), consistent with general cholesterol requirement for clathrin-independent pinocytic pathways (Naslavsky *et al.*, 2004b). Together, these results suggest that at least some of the vacuoles induced by MBCD treatment are macropinosomes. Some MBCD-induced vacuoles may also be

recycling structures: they occasionally moved slowly toward the plasma membrane and fused with it (Fig. 21B).

Caveolin-1-GFP long tubules are microtubule-dependent, Arf6-regulated, and contain EHD proteins and Rab8

The 4-member mammalian cell EHD protein family was identified by homology to *C. elegans* RME-1, which regulates endocytic recycling (Grant *et al.*, 2001). Like RME-1, mammalian EHD proteins act in recycling. They have also been implicated in additional processes, including internalization from the plasma membrane (Naslavsky and Caplan, 2005). EHD proteins share some structural similarity with dynamins, and can tubulate liposomes *in vitro (Daumke et al., 2007)*. As EHD proteins can localize to long microtubule-dependent membrane tubules in several cell types (Caplan *et al.*, 2002; Galperin *et al.*, 2002; George *et al.*, 2007; Roland *et al.*, 2007a), we examined the localization of epitope-tagged EHD1, EHD3, and EHD4 (not shown) in SKBr3 cells. All three proteins were present on membrane tubules in SKBr3 cells (Fig. 22C, D). EHD3 was present on tubules more frequently than EHD1, as reported earlier in other cells (Galperin *et al.*, 2002). All three proteins colocalized with caveolin-1-GFP in punctate structures and also in long tubules when co-expressed in SKBr3 cells (Fig. 22A, B and E).

EHD1- and EHD3- positive tubules are regulated by Arf6, and are not found in cells expressing a constitutively-active Arf6 mutant, Arf6-Q67L (Caplan *et al.*, 2002). Similarly, caveolin-1-GFP-positive long tubules were not seen in cells expressing Arf6-Q67L (not shown). Arf6-Q67L interrupts endocytosis and recycling, and enlarged early endocytic vacuoles accumulate in cells expressing this protein (Naslavsky *et al.*, 2004b). Caveolin-1-GFP accumulated together with Arf6-Q67L in vacuoles in SKBr3 cells, suggesting that it traffics via an Arf6-regulated pathway (Fig. 23).

Rab8 regulates a variety of trafficking events, including transport from the TGN to the plasma membrane (Huber *et al.*, 1993; Peränen *et al.*, 1996; Ang *et al.*, 2003; Sahlender *et al.*, 2005; Sato *et al.*, 2007b) and to lysosomes (del Toro *et al.*, 2009), and also regulates plasma membrane dynamics and cell shape (Peränen *et al.*, 1996; Hattula *et al.*, 2006). Rab8 is present on recycling endosomes (Ang *et al.*, 2003), and may regulate endocytic recycling (Rodriguez and Cheney, 2002; Linder *et al.*, 2007; Roland *et al.*, 2007a). Rab8 can also localize to Arf6-regulated membrane tubules (Hattula *et al.*, 2006), where it can colocalize with EHD proteins (Roland *et al.*, 2007a). Some endogenous Rab8 was present on caveolin-1-GFP-positive tubules in SKBr3 cells (Fig. 24B). Over-expressed wild type GFP-Rab8 and constitutively-active GFP-Rab8-Q67L showed extensive colocalization with caveolin-1-RFP-positive tubules (Fig. 24A). Furthermore, caveolin-1-RFP and GFP-Rab8-Q67L synergized to promote tubule formation.

When expressed individually, GFP-Rab8-Q67L and caveolin-1-RFP were present on long tubules in 12% and 15% of transfected cells respectively. Doubling the amount of each individual plasmid did not significantly increase the fraction of cells with tubules. By contrast, the two proteins were present together on tubules in 30% of co-transfected SKBr3 cells.

Membrane tubules containing EHD proteins and Rab8 are microtubule-dependent (Caplan *et al.*, 2002; Hattula *et al.*, 2006). Similarly, microtubule disruption with nocodazole abolished caveolin-1-GFP long tubules (not shown). Nevertheless, although colocalization of long tubules with microtubules (visualized with co-expressed mCherry tubulin) could occasionally be detected (Fig. 25), it was unusual. This suggested that microtubule-interacting proteins may not be distributed along the length of the membrane tubules.

Together, these results showed that caveolin-1-GFP and caveolin-1-RFP can promote formation of microtubule-dependent, Arf6-regulated plasma membrane-derived tubules that contain EHD proteins and Rab8, and that caveolin-1 and GFP-Rab8-Q67L can synergize to enhance accumulation of these tubules.

Long caveolin-1 membrane tubules do not require actin filaments

To determine whether long tubules required the actin cytoskeleton, we depolymerized actin filaments with latrunculin A (LatA). LatA did not disrupt, and in fact enhanced long tubule formation: abundant tubules were seen in most

transfected cells after LatA treatment (Fig. 26A). (Actin filament depolymerization also greatly enhanced the frequency of Rab8 localization to tubules in Hela cells (Hattula *et al.*, 2006)). As in untreated cells, almost all caveolin-1-GFP long tubules could be labeled by CTxB in 10 min in LatA-treated cells (Fig. 26A). However, additional results showed that caveolin-1 long tubules interacted with and were affected by the actin cytoskeleton. These will be detailed after the following description of short tubules, the second class of caveolin-1-GFP-positive membrane tubules we saw in SKBr3 cells.

Caveolin-1-GFP short tubules depend on the actin cytoskeleton but not on microtubules

Caveolin-1 short tubules were tortuous and highly branched, and were restricted to the zone just under the plasma membrane that also contained the subcortical actin cytoskeleton (Fig. 27A). Short tubules were often closely apposed to actin filaments. Small punctate caveolin-1-positive structures were also abundant in this region, also often in contact with actin filaments (Fig. 27B). Like long tubules, short tubules were endocytic, as they could be labeled by CTxB in 2 min, and by the PI(4,5)P_2-binding probe GFP-PH-PLC-delta, but not by transferrin (Fig. 27C, D and E). Also like long tubules, short tubules were cholesterol-dependent, and were not seen in MBCD-treated cells (Fig. 21A). Unlike long tubules, however, short tubules did not require microtubules, and in

fact appeared more abundant and extensive in nocodazole-treated cells. By contrast, short tubules required actin filaments, and were never seen in cells treated with LatA. Live-cell imaging studies, described next, provided further insights into dynamics and cytoskeletal interactions of long and short tubules.

Caveolin-1-GFP tubules are dynamic

Both long and short tubules were often dynamic, with ends that extended and retracted during observation. Caveolin-1-GFP-positive vacuoles in the cell periphery were sometimes tugged at, presumably by interaction with motors, and tubules sometimes emerged from the vacuoles (Fig. 28). By contrast, vacuoles near the cell center were static (not shown).

Both long and short tubules appeared to be under tension. Segments of long tubules between branch points were usually straight, as if stretched taut (Fig. 29). Both long and short tubules were unstable, and broke down fairly quickly. This occurred when tubules snapped, after which ends retracted (shown for long tubules in Fig. 29 and for short tubules in Fig. 30). In both figures, arrows indicate positions where a tubule will have snapped in the next frame. The resulting tubule fragments often resolved into motile puncta. Short fragments occasionally broke off and moved away from the parent tubule (not shown).

Net tubule length in cells chosen on the basis of abundant tubules decreased substantially over the time of observation.

Although this was true of both long and short tubules, it was easier to quantitate for long tubules. To do this, we examined tubule length in a single cell at two different times, to determine if tubule length decreased over time of observation. Different ways of doing this can be imagined. It's possible that tubules can shrink or disappear by two different mechanisms: one, by retraction and shrinking following breakage, as we observed, and a second, in which tubules would disappear rapidly be a second mechanism. Ideally, to control for this possibility, one might examine individual tubules in a cell, and measure the decrease in length, or alternatively the disappearance, of each tubule over time. However, we observed that over 10 minutes of observation, many tubules decreased gradually in length, but disappeared by the end of the observation time. In addition, as the cell moved during the observation time, individual tubules often came into focus, or moved out of the focal plane. Thus, following individual tubules over time was technically problematic. For this reason, we used an alternate approach to quantitation. We were primarily interested in the net change in the length of long tubules over the period of 10 minutes, without regard to the specific mechanism of the change. Thus, we measured total tubule length (in one focal plane) per cell in a frame captured at the start of observation, and another frame of the same cell taken 10 min later. We note that this method does not give information on how many mechanisms of tubule loss operate. Total

tubule length at the start varied widely between cells (from 30 to 200 μm), but decreased by a fairly uniform 70-80% over 10 min (Table 1).

Actomyosin interactions exert tension on long tubules

Although LatA did not disrupt long tubules, it affected their morphology and behavior. Tubule ends remained highly dynamic in LatA-treated cells, showing that they continued to interact with microtubule-dependent motors. In contrast to control cells, long tubules in LatA-treated cells often had a curved, flaccid appearance, suggesting they were under less tension than tubules in control cells (Fig. 31A). (A section of the control cell (Fig. 31B) shown in Fig. 18A is shown for comparison). Furthermore, live cell imaging showed that long tubules in LatA-treated cells rarely snapped, and did not decline in abundance over the time of observation (Table 1). Together, these results suggested that long tubules interacted with actin filaments as well as microtubules, and that interactions with the actin cytoskeleton induced strain on the tubules and enhanced their breakdown. Visualization of F-actin in a cell containing long tubules supported this idea (Fig. 32). Caveolin-1-positive puncta and short tubules were often seen to associate closely with actin filaments just below the plasma membrane. By contrast, long tubules extended deeper into the cell, beyond the zone containing the cortical actin cytoskeleton. Nevertheless,

apparent points of contact between long tubules and cortical actin filaments were sometimes seen (arrows in Fig. 32).

By contrast, short tubules in nocodazole-treated cells were similar to controls with respect to morphology, snapping and retraction, and net loss over the time of observation. This suggested that dynamics and stability of short caveolin-1-GFP-positive tubules were not affected by interaction with microtubules. Instead, these results suggested that actin cytoskeleton interactions affected dynamics and stability of short tubules as well as long ones.

Myosin II is responsible for cortical tension in the actomyosin cytoskeleton (Clark *et al.*, 2007). To determine whether myosin II exerted tension on caveolin-1 long tubules, we examined tubule stability in cells treated with the myosin II inhibitor blebbistatin. As blebbistatin induces phototoxicity in live cells expressing GFP-tagged proteins (Kolega, 2004), we expressed caveolin-1-RFP in these experiments. Rapid bleaching of RFP made tubule dynamics harder to visualize than in cells expressing caveolin-1-GFP. Nevertheless, caveolin-1-RFP tubules showed similar behavior to caveolin-1-GFP tubules. Tubules snapped, and tubule length decreased over time (Table 1). By contrast, tubule snapping was not observed in blebbistatin-treated cells, and tubules remained stable (Table 1). We conclude that myosin II induces tension on caveolin-1-positive membrane tubules.

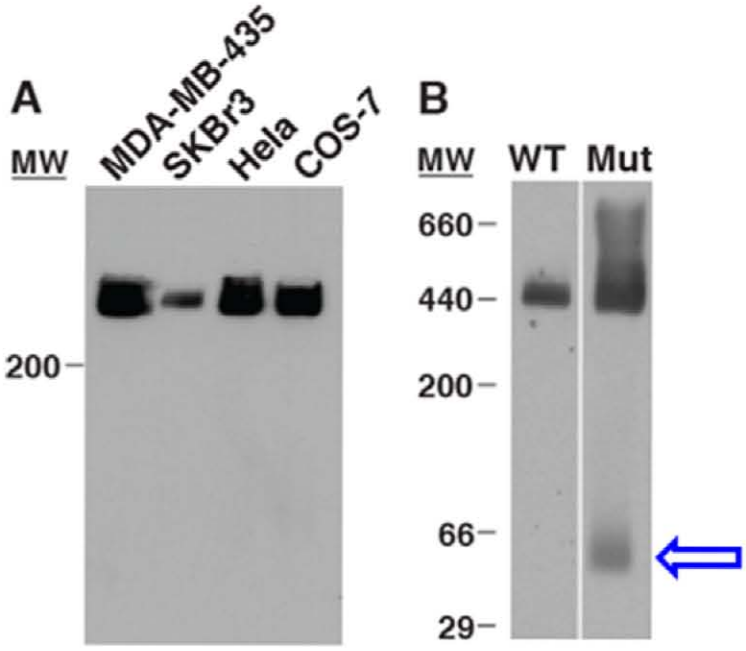
A
MW
MDA-MB-435
SKBr3
Hela
COS-7
200
B
MW
WT
Mut
660
440
200
66
29

Figure 11. Caveolin-1 oligomerizes normally in SKBr3 cells. (A) Proteins in lysate of SKBr3, MDA-MB-435, Hela and COS-7 cells transfected with wild-type caveolin-1 were separated by blue native gel electrophoresis and transferred to PVDF membranes. Caveolin-1 was detected by Western blotting. (B) Oligomerization of caveolin-1 compared to the caveolin-1 mutant (caveolin-102A5) that does not oligomerize fully. Positions of molecular weight standards (MW), detected by Coomassie Blue staining of the membrane, are shown. The arrow indicates the position of monomer on the gel.

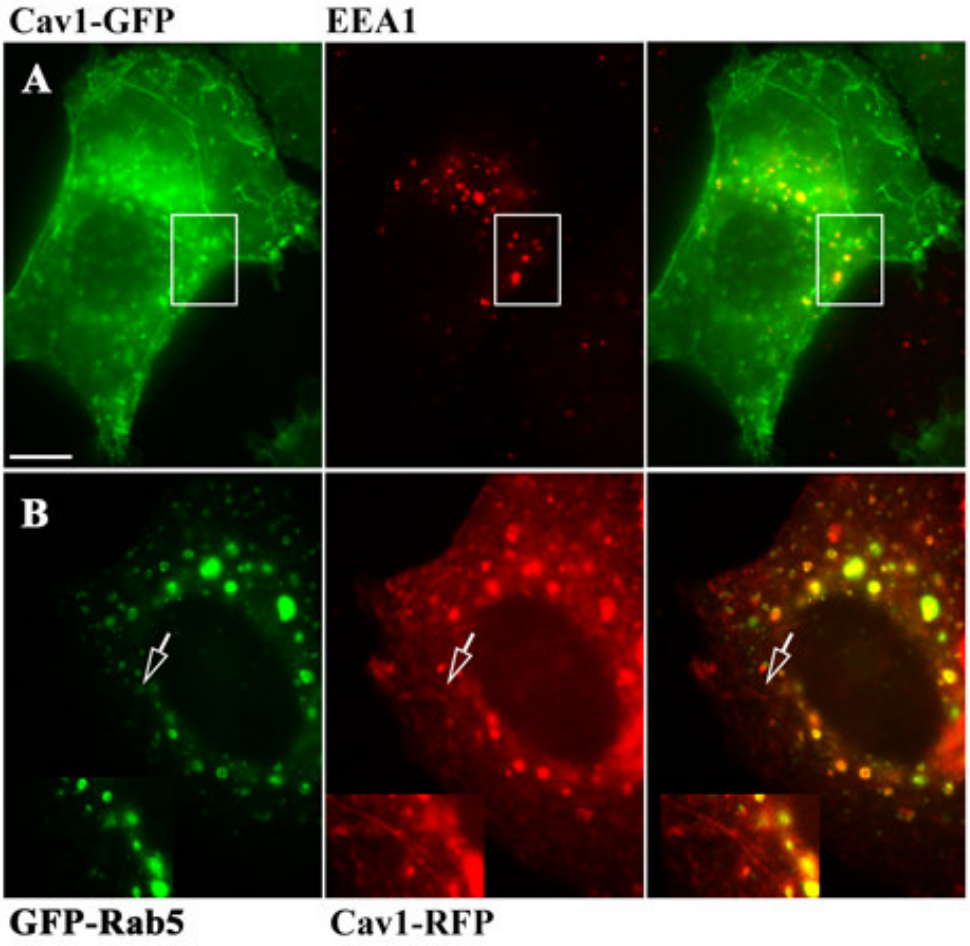
Cav1-GFP
EEA1
A
B
GFP-Rab5
Cav1-RFP

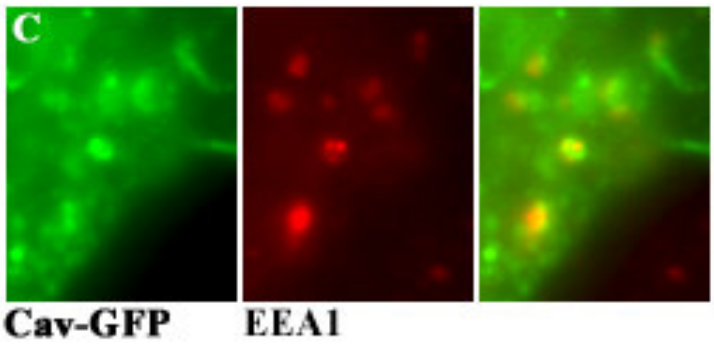
C
Cav-GFP
EEA1

Figure 12. Caveolin-1 localizes in punctate structures and early endosomes in cytoplasm. Rab5 increases localization of caveolin-1 in early endosomes. SKBr3 cells were transiently transfected with caveolin-1-GFP alone (A) or with caveolin-1-RFP and constitutively active GFP-Rab5 (B). Cells were fixed, permeabilized and EEA1 was detected by immunofluorescence. The higher magnification of the regions marked by arrow in (B) is shown at the lower left corner of the panel. The boxed area in (A) is magnified in (C). Right-hand panels in A and B show merged images. All images are epifluorescence images. Scale bar; A, 5 μm, applies to all.

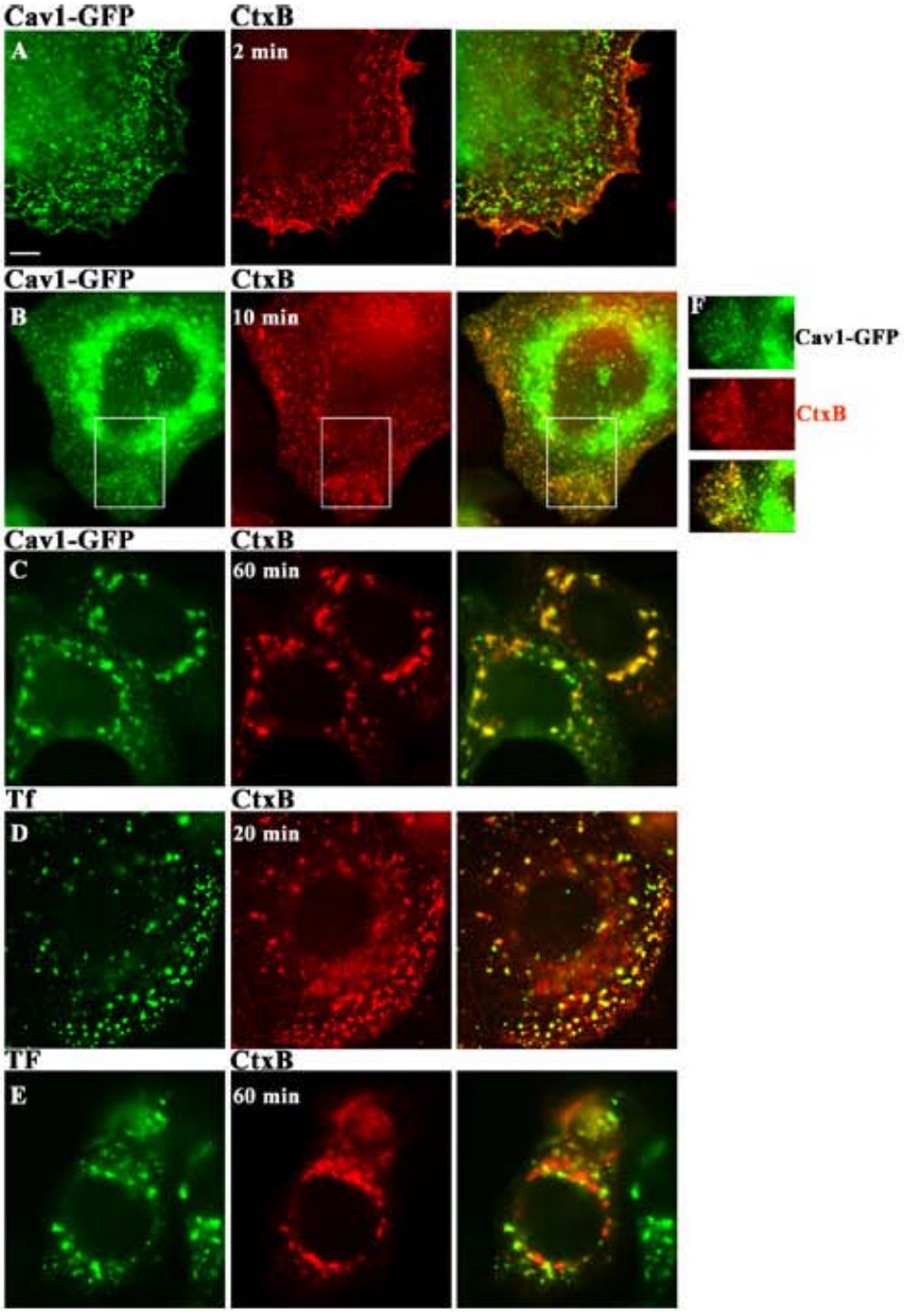
Cav1-GFP
CtxB
A
2 min
Cav1-GFP
CtxB
B
10 min
F
Cav1-GFP
CtxB
Cav1-GFP
CtxB
C
60 min
Tf
CtxB
D
20 min
TF
CtxB
E
60 min

Figure 13. Caveolin-1 positive structures are endocytic. SKBr3 cells were transiently transfected with caveolin-1-GFP (A-C). Cells were incubated with either AF-594-CtxB (0.5 µg/ml) alone (A, B) or with AF-594-CtxB and FITC-Tf (50 µg/ml) (C, D) for the indicated time in the panel. Cells were then fixed and permeabilized. All images are epifluorescence images (A-E). Merged images are shown in right-hand panels in A-E and in bottom panel in F. The boxed area in panel B is enlarged in panel F to show colocalization. Scale bar; A, 5 µm, applies to all.

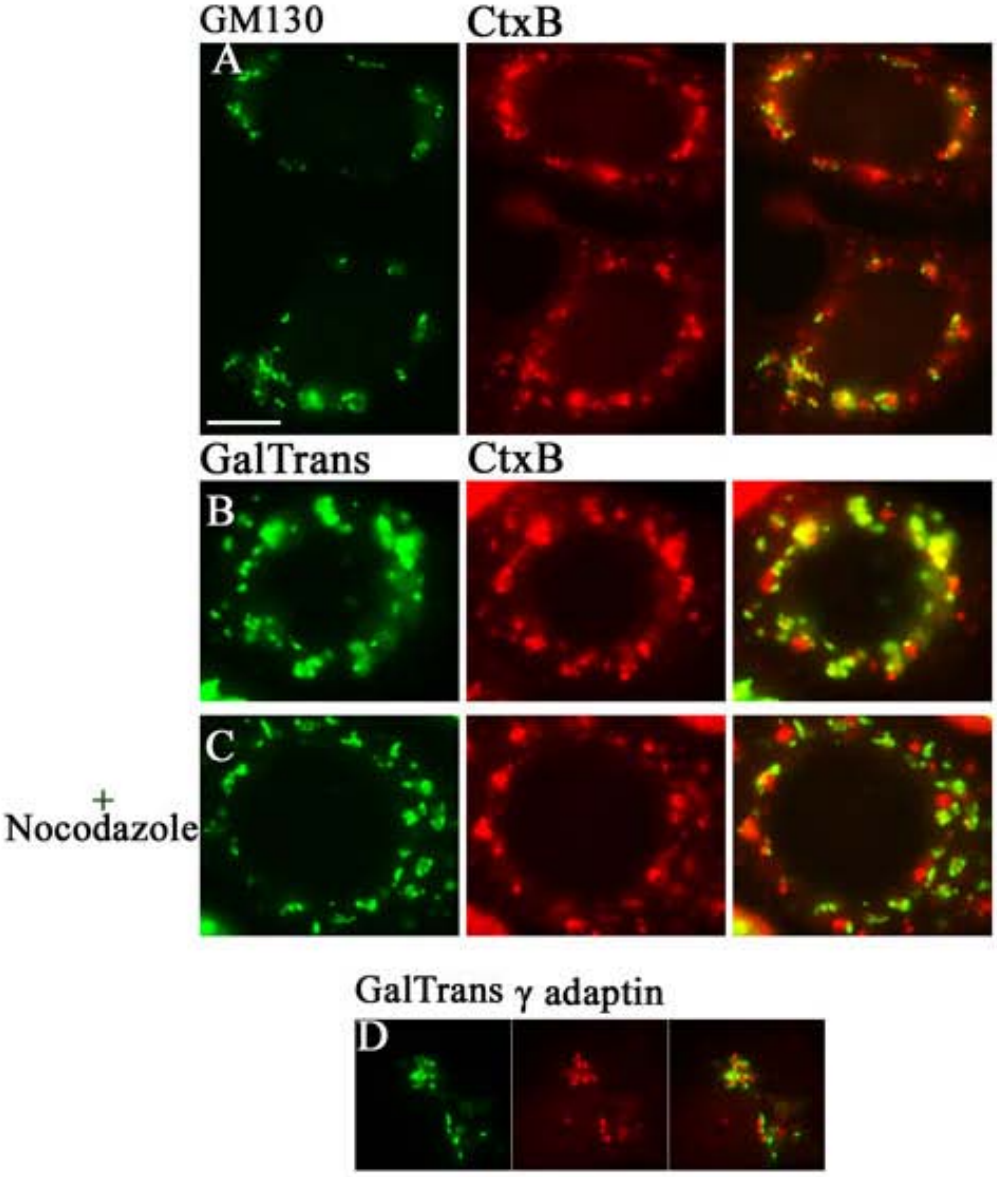
GM130
CtxB
A
GalTrans
CtxB
B
C
+
Nocodazole
GalTrans γ adaptin
D

Figure 14. CtxB localizes to a compartment distinct from trans and cisternal Golgi markers. SKBr3 cells were transiently either transfected with YFP-GalTrans (B-D) or left untransfected (A). Cells in panel (C) were pre-treated with nocodazole (10 µm) for 2 hours at 37°C. AF-594-Ctxb (0.5 µg/ml) was bound to cells for 60 minutes at 37°C (A-C). Nocodazole was added with AF-594-CtxB for the cells in panel (C). Cells were fixed, permeabilized and GM130 and γ-adaptin were detected by immunofluorescence. All images are epifluorescence (A-D). Merged images are shown in right-hand panels in A-D. Scale bar; A, 10 µm, applies to all.

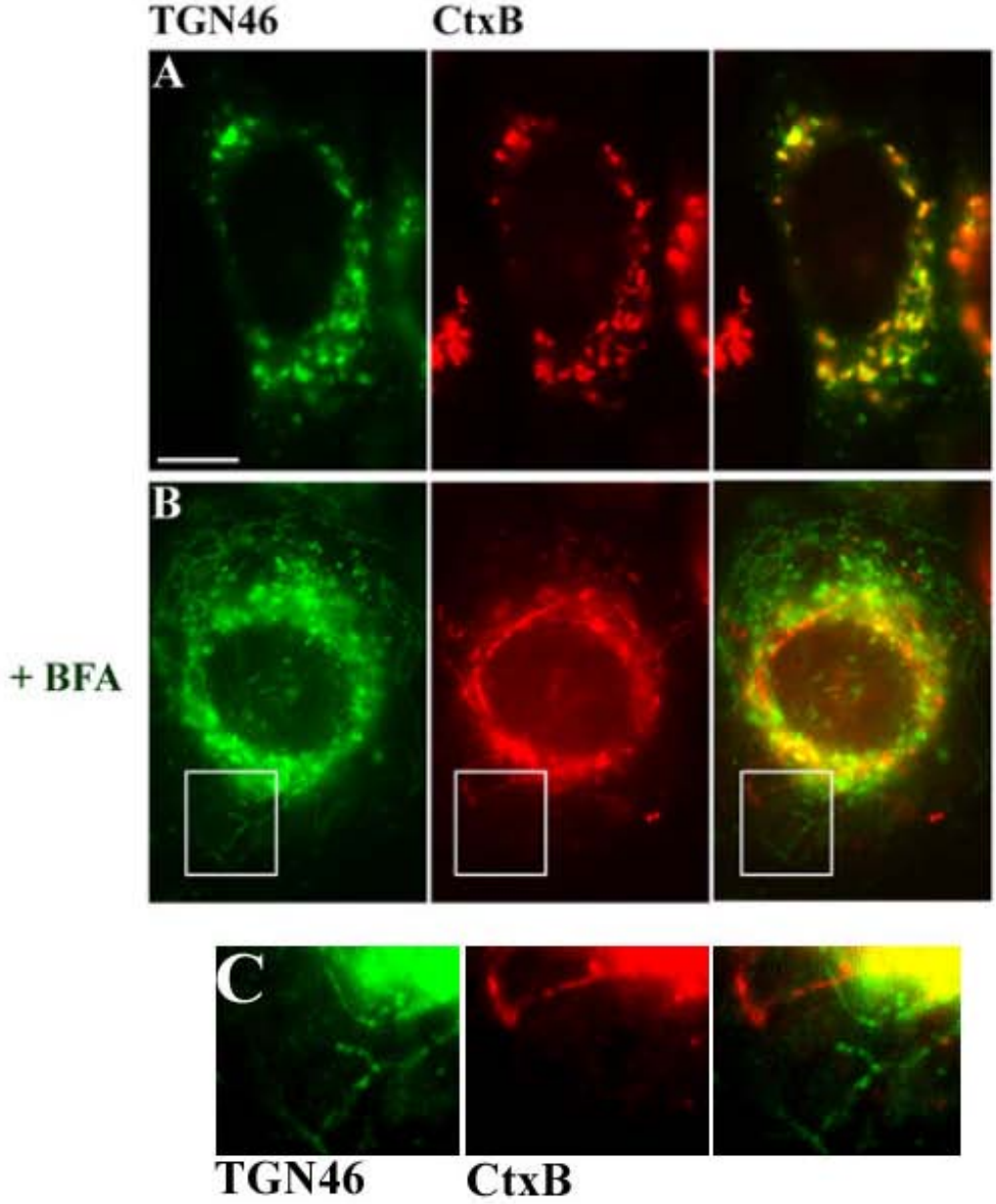
TGN46
CtxB
A
B
+ BFA
C
TGN46
CtxB

Figure 15. Effect of brefeldin A treatment on localization of CtxB and TGN46 (taken from Catherine Peterson, Brown lab). Cells were incubated in media containing AF-594-CtxB (0.5 µg/ml) alone (A) or AF-594-CtxB and brefeldin A (50 µg/ml) together (B) for 60 minutes at 37°C. TGN46 was visualized by immunofluorescence. All images are epifluorescence. Merged images are shown in right-hand panels in A and B. The boxed area in (B) is enlarged in panel (C). Scale bar; A, 10 µm, applies to all.

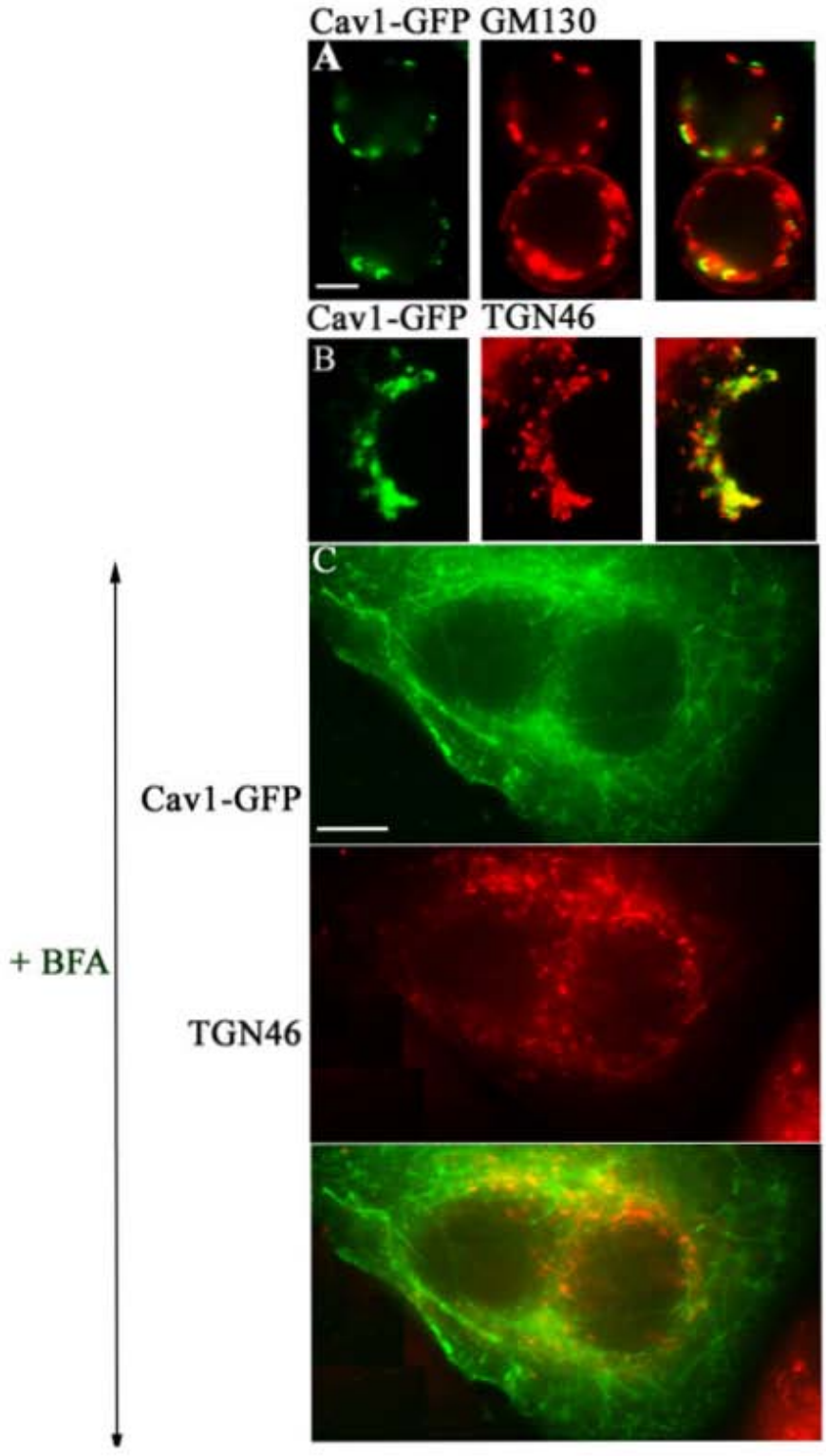
Cav1-GFP GM130
A
Cav1-GFP TGN46
B
C
Cav1-GFP
+ BFA
TGN46

Figure 16. Like CtxB, caveolin-1 does not colocalize with TGN46, even after brefeldin A treatment (taken from Catherine Peterson, Brown lab). . SKBr3 cells were transiently transfected with caveolin-1-GFP (A-C). Cells were pre-treated with brefeldin A (50 µg/ml) for 1 hour at 37°C. Cells were fixed, permeabilized and GM130 and TGN46 were detected by immunofluorescence. All images are epifluorescence (A-C). Merged images are shown in right-hand panels in A, B and in bottom panel in C.

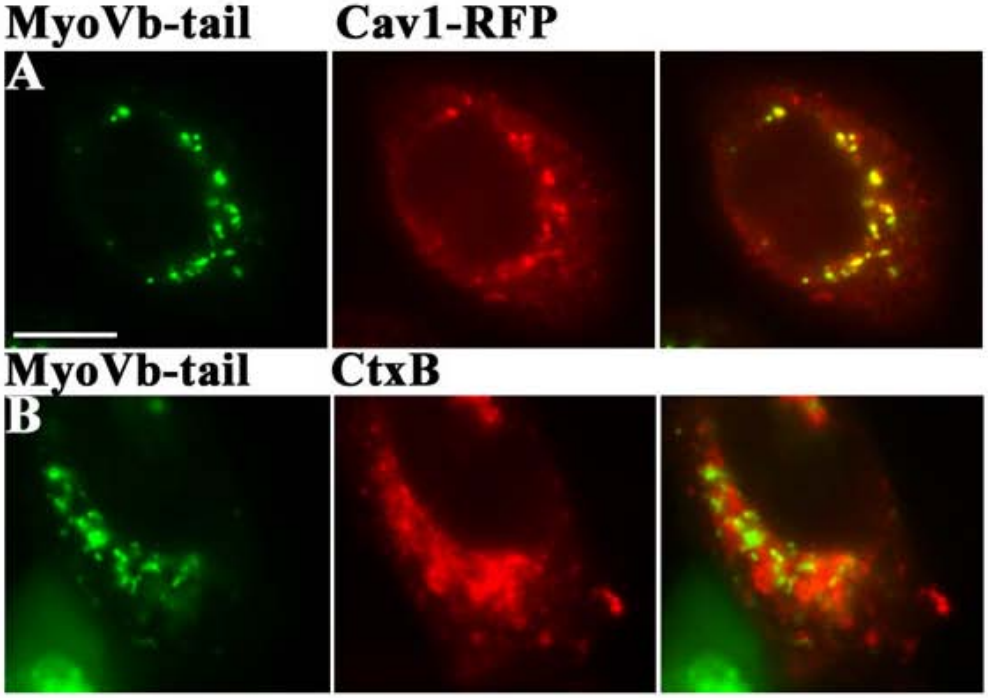
MyoVb-tail
Cav1-RFP
A
MyoVb-tail
CtxB
B

Figure 17. Myosin Vb tail traps caveolin-1 but not CtxB in perinuclear structures. SKBr3 cells were transiently transfected with GFP-myosin Vb tail alone (B) or with caveolin-1-RFP and GFP-myosin Vb tail (A). Cells in panel (B) were incubated in media containing AF-594-CtxB (0.5 μg/ml) for 60 minutes at 37°C. Cells were then fixed, permeabilized and processed for immunofluorescence. All are images are epifluorescence. Merged images are shown in right-hand panels in A and B. Scale bar; 10 μm, applies to all panels.

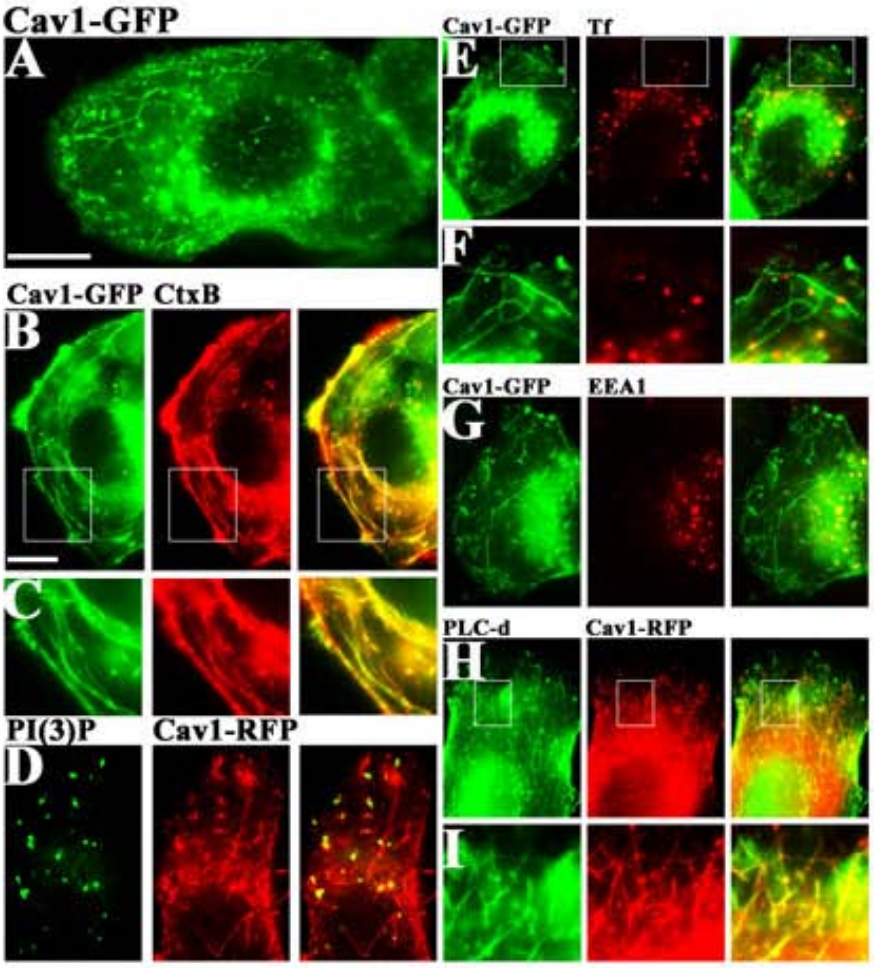
Cav1-GFP
A
Cav1-GFP CtxB
B
C
PI(3)P
Cav1-RFP
D
Cav1-GFP
Tf
E
F
Cav1-GFP
EEA1
G
PLC-d
Cav1-RFP
H
I

Figure 18. Caveolin-1 forms endocytic tubular structures in SKBr3 cells which do not colocalize with early endosomes ((D, H) taken from Anne Ostermeyer-Fay, Brown lab). . SKBr3 cells were transiently transfected with caveolin-1-GFP (A, B, E and G), caveolin-1-RFP and either GFP-tagged PLC-δ PH domain (A) or GFP-FYVE domain (D). Cells were incubated with AF-594-CtxB (0.5 µg/ml) (B) and FITC-Tf (50 µg/ml) (E) for 10 and 5 minutes at 37^{o}C respectively. Cells were fixed, permeabilized and EEA1 was visualized by immunofluorescence. The right-side images are the merged images (A-I). The boxed area in B, E and H are blown up in C, F and I, respectively. All images are epifluorescence. Scale bars; A, 10 µm; B (applies to B-I) 5 µm

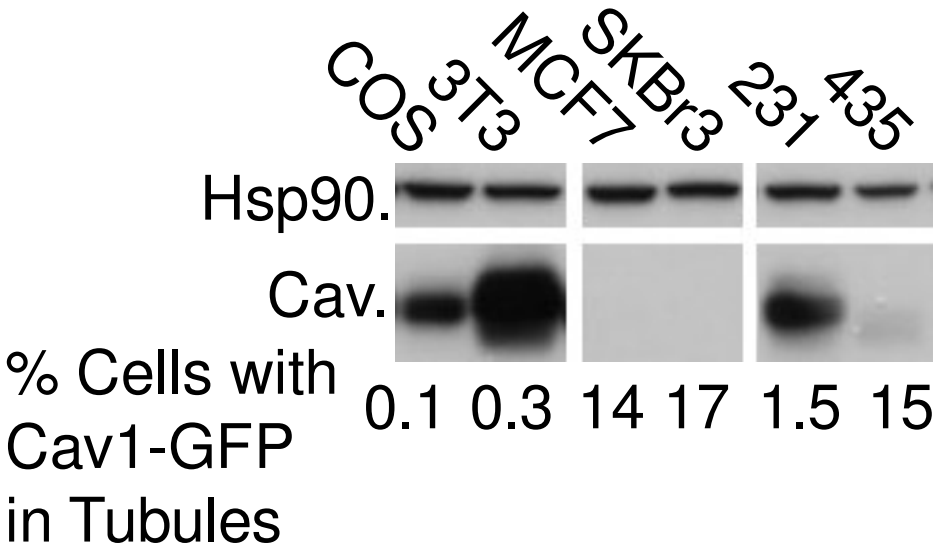
COS
3T3
MCF7
SKBr3
231
435
Hsp90.
Cav.
% Cells with Cav1-GFP in Tubules
0.1 0.3 14 17 1.5 15

Figure 19. Tubular localization of exogenous caveolin-1 in different cell lines correlates inversely with expression of endogenous caveolin-1. SKBr3, NIH3T3, COS7, MCF-7, MDA-MB-231, MDA-MB-435 cells were lysed in gel loading buffer and protein were separated by SDS-PAGE and transferred to a membrane for Western blotting analysis. Caveolin-1 and HSP90 were detected by using the respective antibodies. To determine the percentage of cells with tubules, 120 cells were randomly counted on the slide with fixed cells. The number of cells with either long or short tubules was converted to percentage. The final percentage is the average of three different counts done on different set of cells.

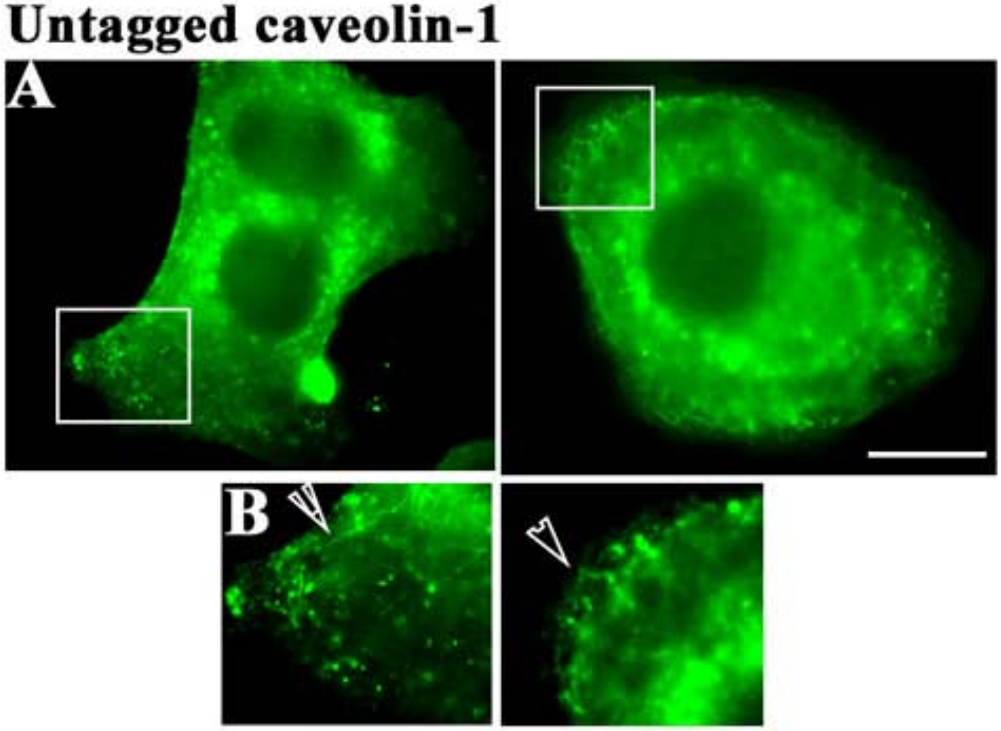
Untagged caveolin-1
A
B

Figure 20. Tubular localization of untagged caveolin-1 in SKBr3 cells. SKBr3 cells were transiently transfected with caveolin-1-GFP (A). Cells were fixed, permeabilized and caveolin-1 was visualized by immunofluorescence using polyclonal anti-caveolin-1 antibody. The boxed areas in A are blown up in B. The arrowhead points to a tubules (B). All images are epifluorescence. Scale bars; A, 10 μm, applies to all.

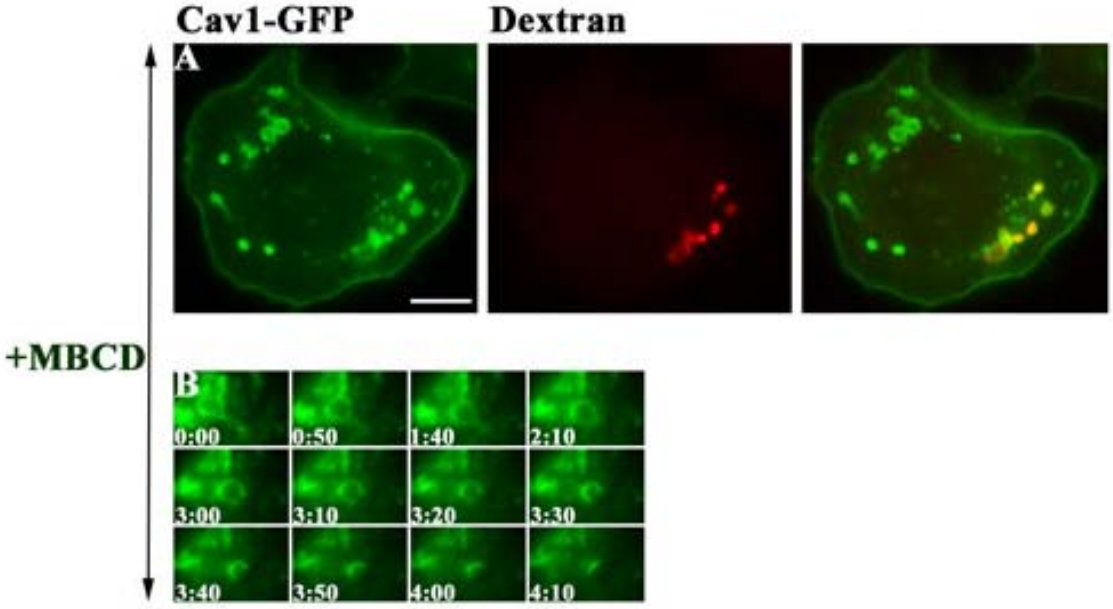
Cav1-GFP
Dextran
A
+MBCD
B
0:00
0:50
1:40
2:10
3:00
3:10
3:20
3:30
3:40
3:50
4:00
4:10

Figure 21. Caveolin-1 tubules are dependent on cholesterol. SKBr3 cells were transiently transfected with caveolin-1-GFP (A and B). Cells were pre-treated with serum free media containing 10 mM MBCD for 45 minutes at 37^{o}C (A and B) followed by incubation in media with 10 mM methyl-β-cyclodextrin (MBCD) and 1 mg/ml FluoroRuby dextran for 10 minutes (A). Cells were then fixed, permeabilized and processed for immunofluorescence (A). Merged images are on the right of the panel (A). The selected frames from the time-lapse recording of SKBr3 cells plated on a glass bottom dish are shown (B). For the recording cells were maintained in serum free media with MBCD. A total of 4 minutes and 10 seconds recording is shown. The time indicated on each frame shows the time elapsed since the first frame was taken. The images in (B) shows a caveolin-1-GFP vacuole fusing with plasma membrane in cells treated with MBCD as mentioned above. The arrowhead in (B) points to a vacuole that fuses with plasma membrane in subsequent panels. Scale bar; 10 μm

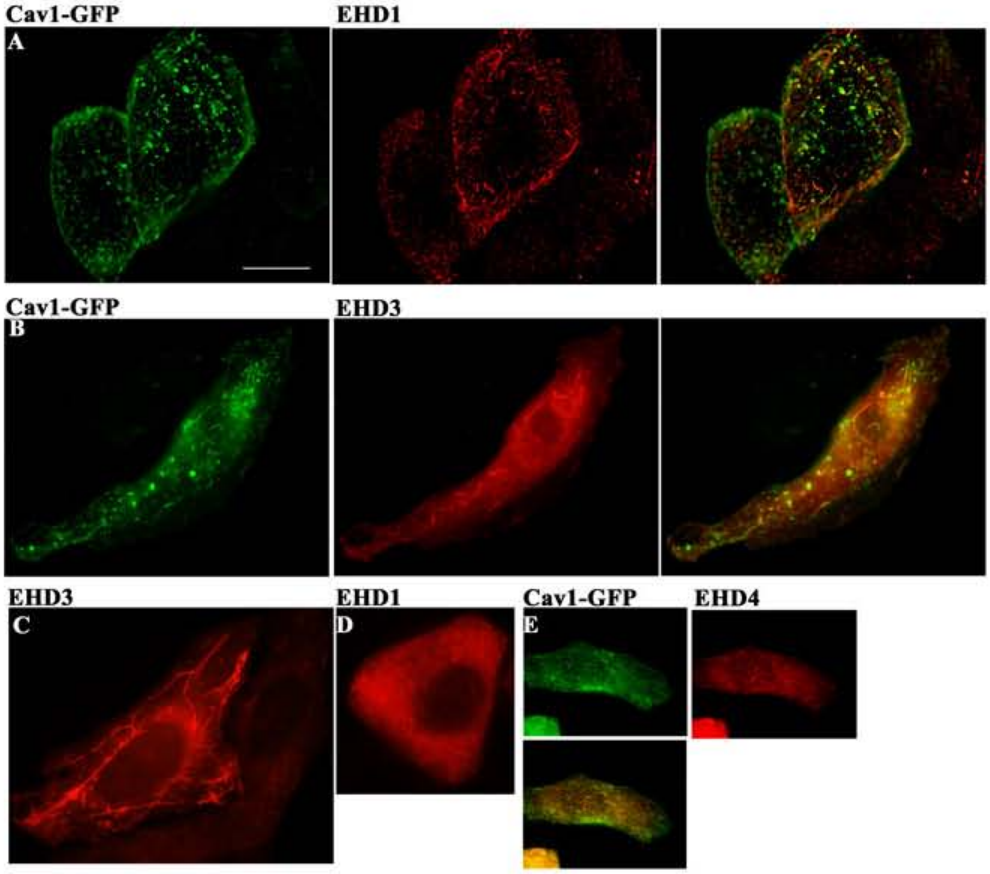
Cav1-GFP
EHD1
A
Cav1-GFP
EHD3
B
EHD3
EHD1
Cav1-GFP
EHD4
C
D
E

Figure 22. Caveolin-1 tubules colocalizes with the tubules of EHD proteins. SKBr3 cells were transiently transfected with caveolin-1-GFP and EHD1 (A), EHD3 (B), or EHD4 (E), while the cells in panel (C) and (D) were transiently transfected with either EHD3 (C) or EHD1 (D) only. Cells were fixed, permeabilized and EHD proteins were detected using anti-myc tag antibody. Deconvolved images from *z*-stacks are shown (A-D) with the merged images on the right-hand panels (A and B). Images in (E) are epifluorescence with the merged image at the bottom. Scale bar; 10 μm

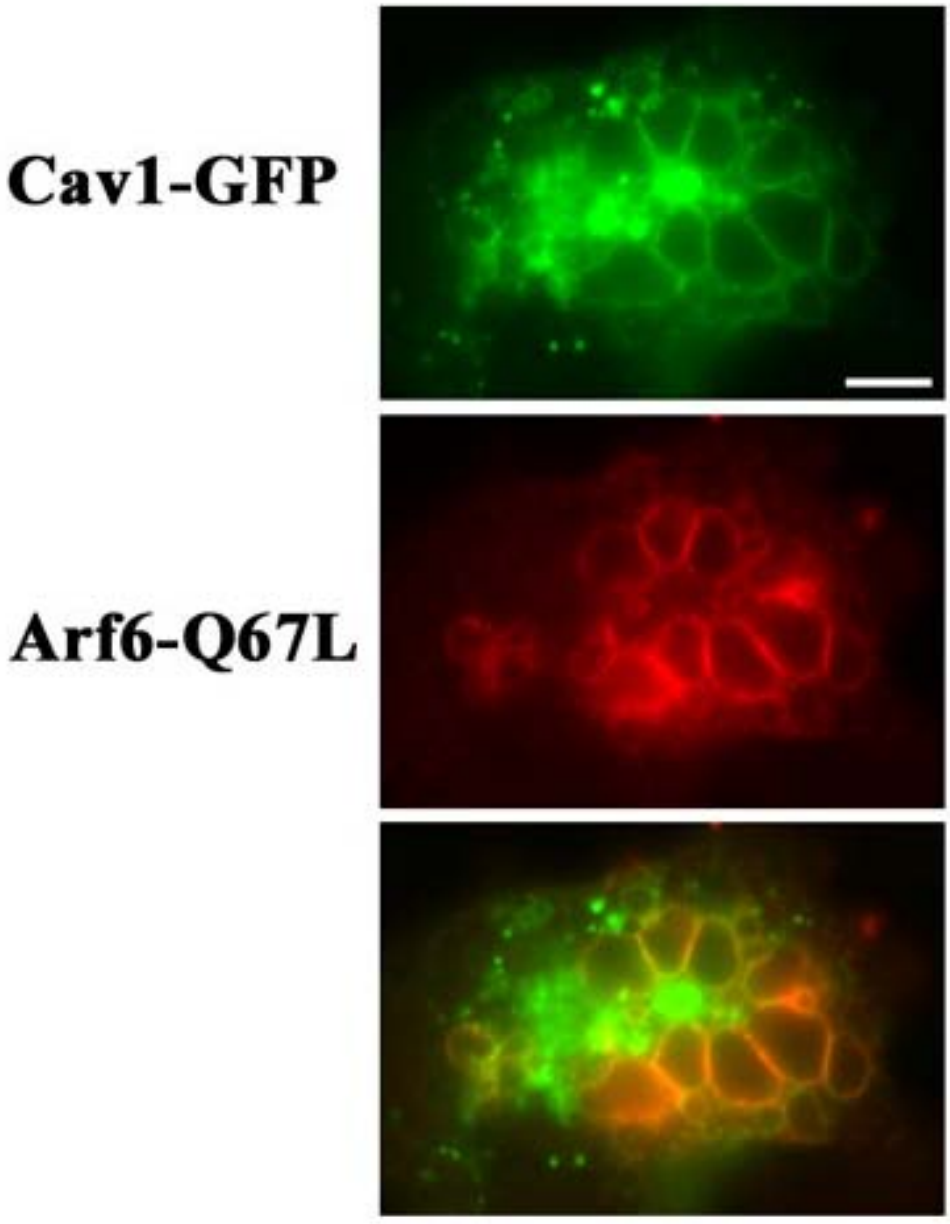
Cav1-GFP
Arf6-Q67L

Figure 23. Effect of Arf6Q67L on the localization of caveolin-1. SKBr3 cells were transiently transfected with caveolin-1-GFP and constitutively active HA-Arf6-Q67L. Cells were fixed, permeabilized and processed for immunofluorescence. Arf6 was detected by rabbit anti-HA antibody. Epifluorescence images are shown with the merged image at the bottom. Scale bar; 5 μm

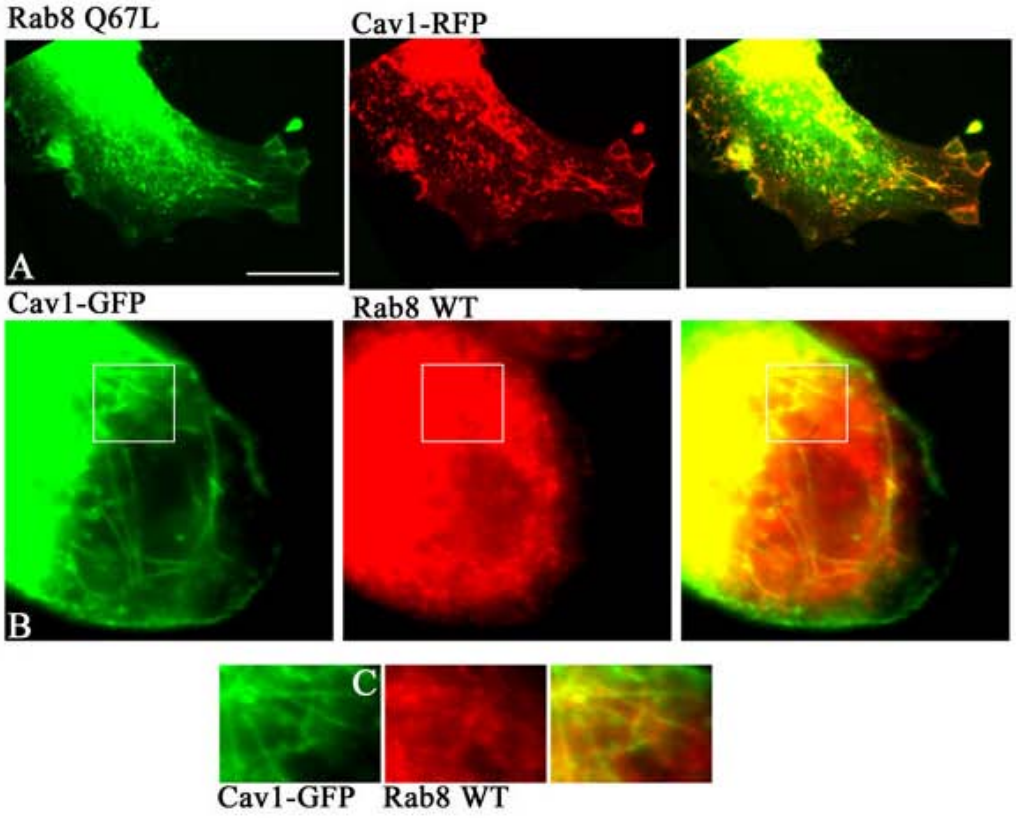
Rab8 Q67L
Cav1-RFP
A
Cav1-GFP
Rab8 WT
B
C
Cav1-GFP
Rab8 WT

Figure 24. Endogenous wild type Rab8 showed some colocalization with caveolin-1, while over-expressed wild type and constitutively active Rab8 Q67L showed extensive colocalization with caveolin-1 in puncta and tubules. SKBr3 cells were transfected with caveolin-1-RFP and constitutively active GFP-Rab8-Q67L (A) or with caveolin-1-GFP alone (B). Cells were fixed, permeabilized for immunofluorescence. Wild type Rab8 was detected by monoclonal anti-Rab8. The boxed section in (B) is enlarged shown in (C). Merged images are on the right. All images are epifluorescence. Scale bar: 10 μm

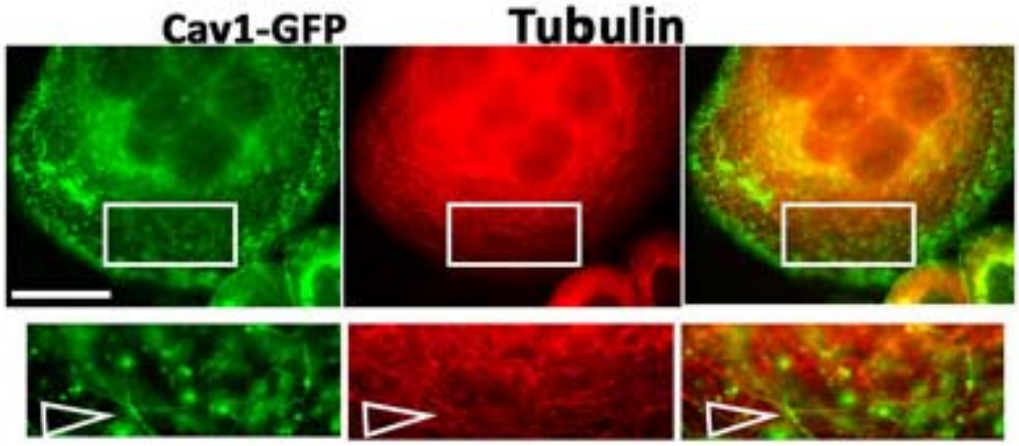
Cav1-GFP
Tubulin

Figure 25. Colocalization of caveolin-1 tubules with the microtubules. SKBr3 cells were transiently co-transfected with caveolin-1-GFP and mCherry tubulin. Cells were then fixed, permeabilized and examined by epifluorescence microscope. The merged image is on the right. The boxed area in top panel is enlarged in the bottom panel. The arrowhead points to a caveolin-1-GFP tubule in close association with a microtubule.

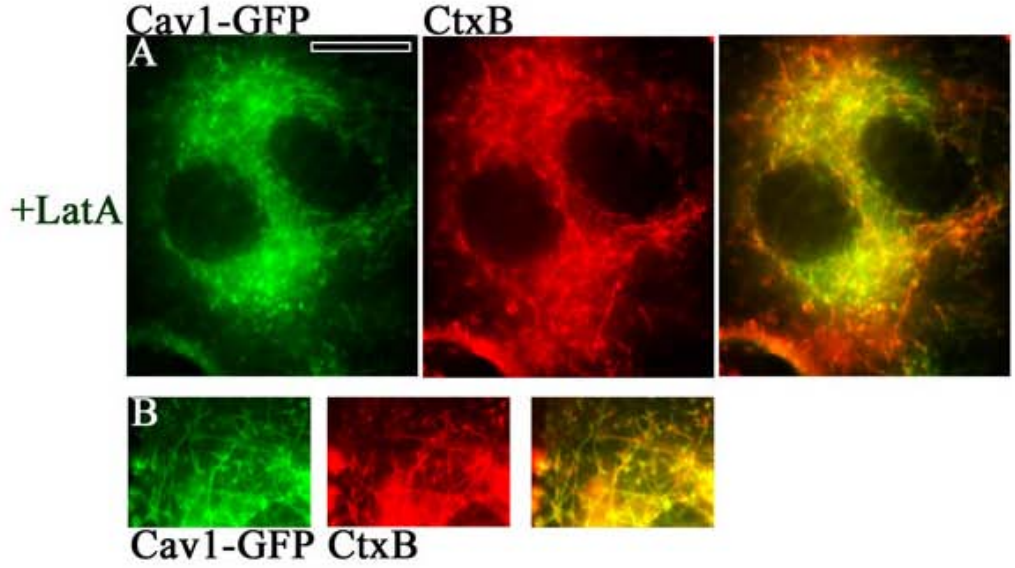
Cav1-GFP
CtxB
A
+LatA
B
Cav1-GFP
CtxB

Figure 26. Effect of latrunculin A on the tubular localization of caveolin-1. SKBr3 cells transiently transfected with caveolin-1-GFP were pretreated with latrunculin A (LatA) (5 µm) for 30 minutes at 37°C. Cells were then incubated in media containing LatA (5 µm) and AF-594-CtxB (0.5 µg/ml) for 10 minutes at 37°C. Cells were then fixed, permeabilized and imaged with epifluorescence microscope. The merged images are on the right-hand panels (A and B). The enlarged portion of the white box in (A) is shown in B. Scale bar; 10 µm

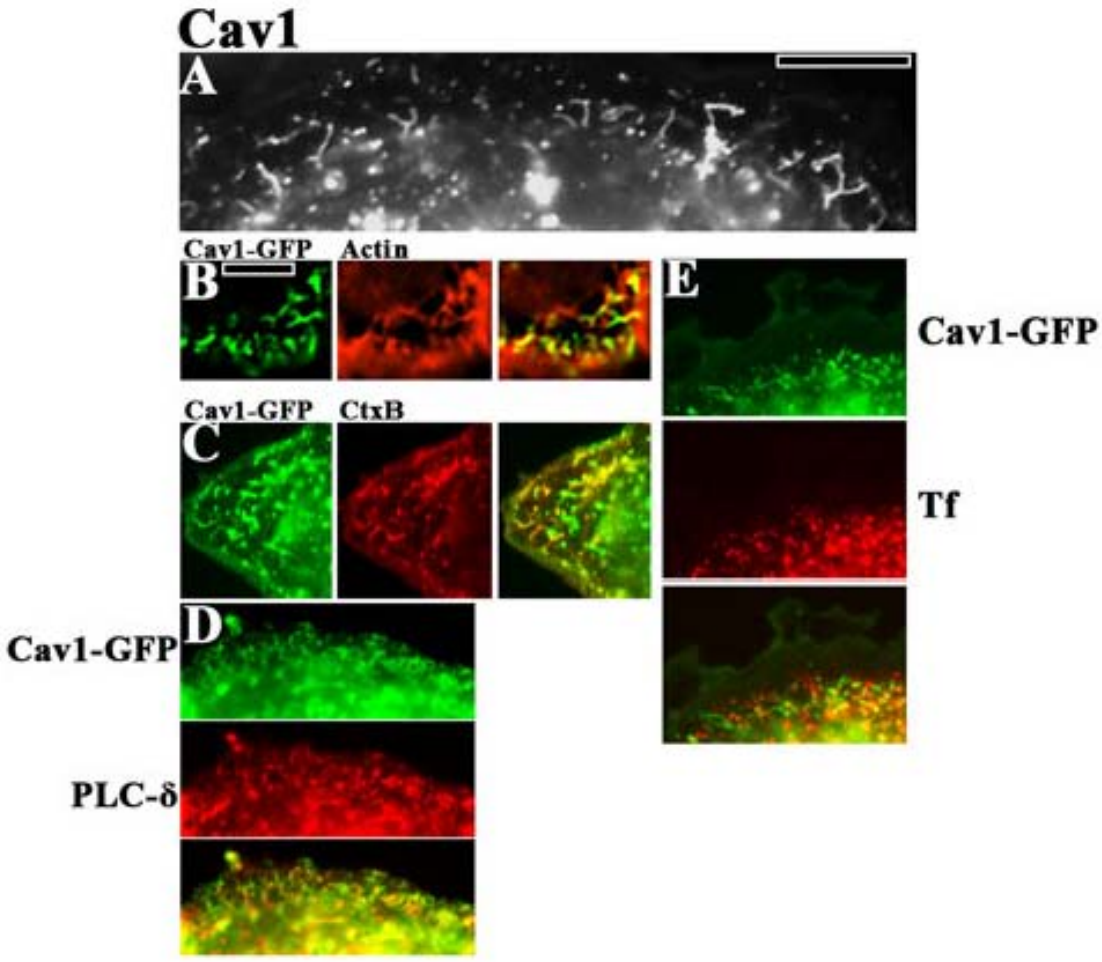
Cav1
A
Cav1-GFP
Actin
B
Cav1-GFP
CtxB
C
Cav1-GFP
D
PLC-δ
E
Cav1-GFP
Tf

Figure 27. Short tubules of caveolin-1 colocalize with actin and like long tubules, are endocytic ((D) taken from Anne Ostermeyer-Fay, Brown lab). SKBr3 cells transiently expressing caveolin-1-GFP (A-C and E), caveolin-1-GFP and GFP-tagged PLC-δ PH domain (D only) were incubated with AF-594-CtxB (0.5 µg/ml) for 2 minutes at 37°C (C only), FITC-Tf (50 µg/ml) for 5 minutes at 37°C (E only). Cells were fixed and permeabilized. Actin in (B) was visualized by using AF-594-phalloidin. Scale bars; A, 10 µm; B (applies to B-E) 5 µm

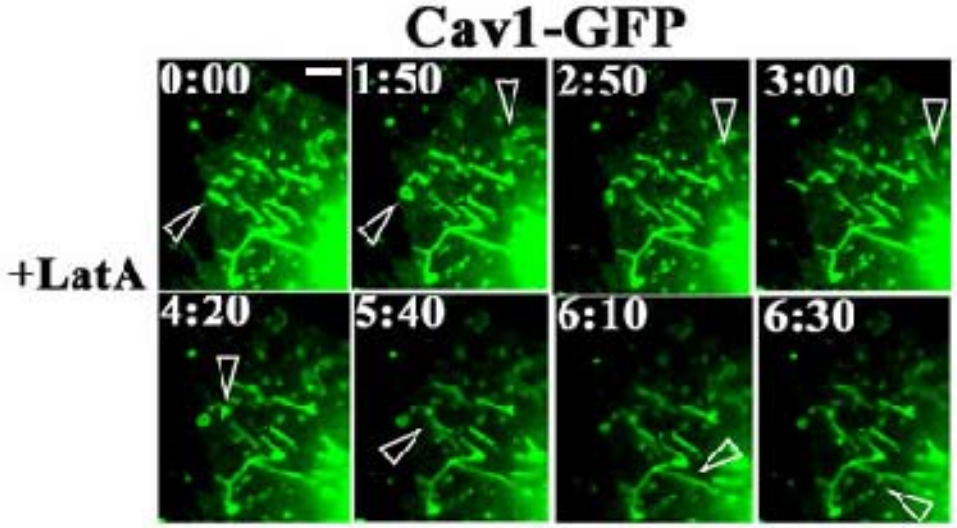
Cav1-GFP
+LatA
0:00
1:50
2:50
3:00
4:20
5:40
6:10
6:30

Figure 28. The short and long tubules of caveolin-1 are highly dynamic. SKBr3 cells were grown on glass bottom dishes and transiently transfected with caveolin-1-GFP. After 48 hours post-transfection, cells were incubated in media containing LatA (5 μm) for 90 minutes before recording the movie with the frame interval of 10 seconds. Series of selected frames are shown with the time stamps indicated. The time (min:sec) on each frame indicates the time since the first frame was taken. The arrow marks the tubule or a vacuole displaying the stretching and snapping. Scale bar (applies to all panels); 5 μm.

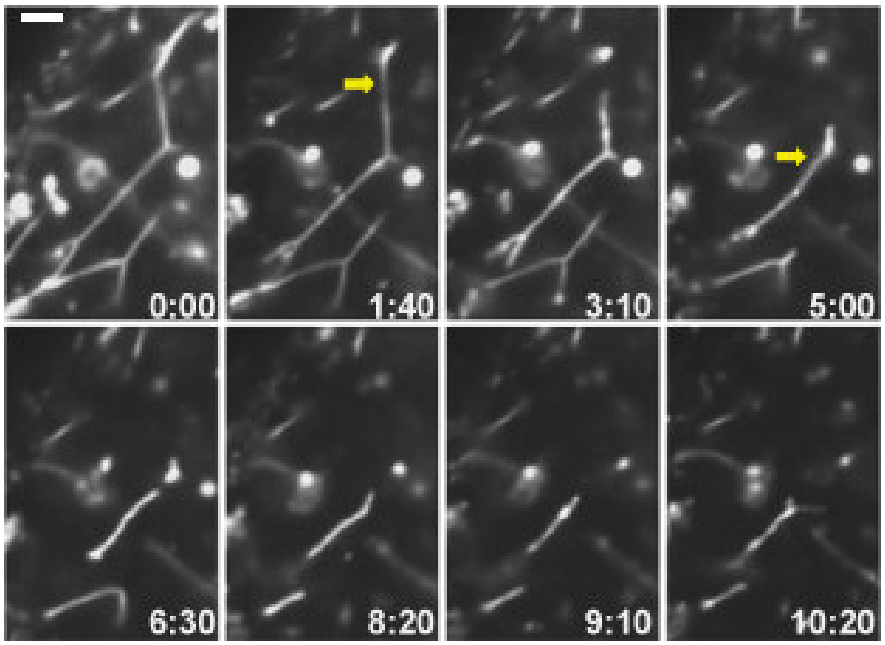
0:00
1:40
3:10
5:00
6:30
8:20
9:10
10:20

Figure 29. Long tubules appear to be under tension and snap into a punctate structure. SKBr3 cells grown on glass bottom dishes, transiently expressing caveolin-1-GFP, were processed for live-cell recordings. Selected frames are shown with the arrows pointing at the long tubules that subsequently snap into a punctate structure. Time is shown in min:sec. Scale bar (applies to all panels); 5 μm.

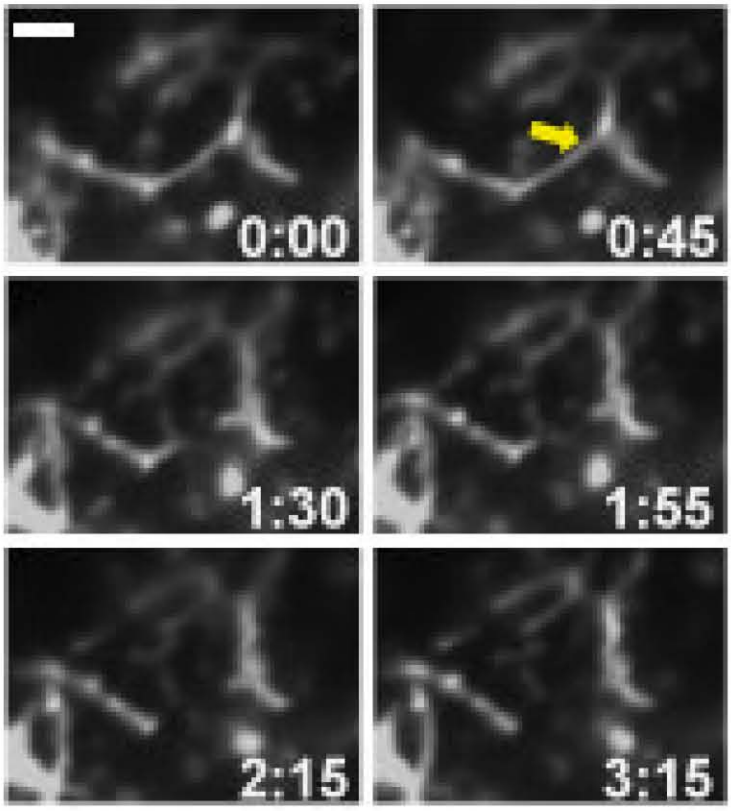
0:00
0:45
1:30
1:55
2:15
3:15

Figure 30. Like long tubules, short tubules exhibit rich dynamics, snapping into a punctate structure. Still images from the live-cell recording of SKBr3 cells transiently expressing caveolin-1-GFP are shown with time stamps (min:sec). The arrow points to a short tubule that subsequently snaps into a punctate structure. Scale bar (applies to all panels); 5 μm.

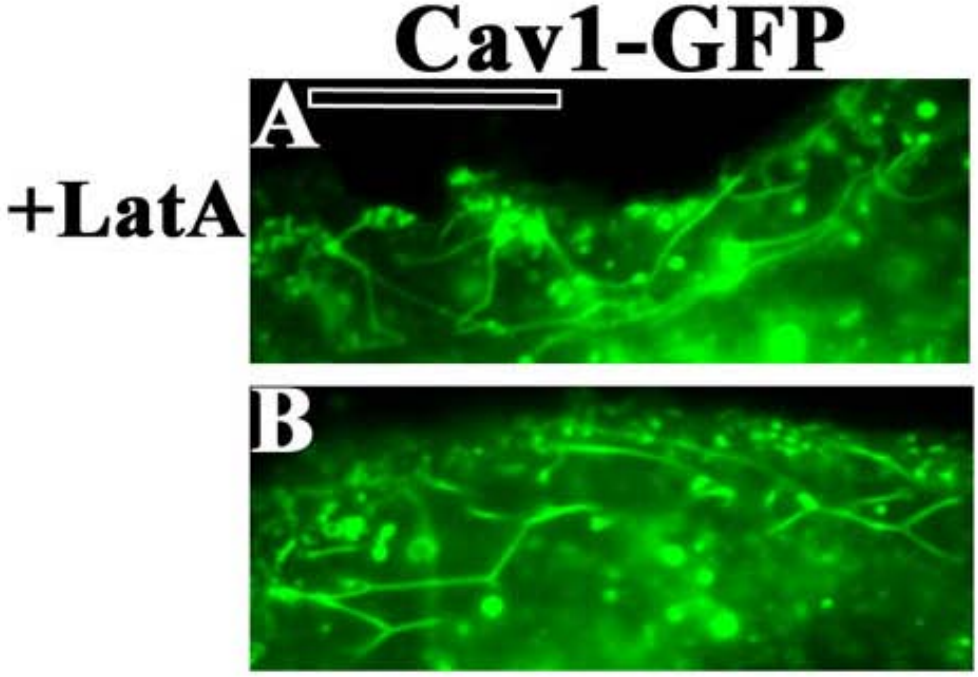
Cav1-GFP
+LatA
A
B

Figure 31. Latrunculin A treatment reduces the tension on long tubules of caveolin-1. SKBr3 cells transiently expressing caveolin-1-GFP were pre-treated with latrunculin A (5 μm) for 30 minutes at 37°C (A) or left untreated (B). A still frame from a time lapse recording is shown (A). Scale bar (applies to all panels); 5 μm.

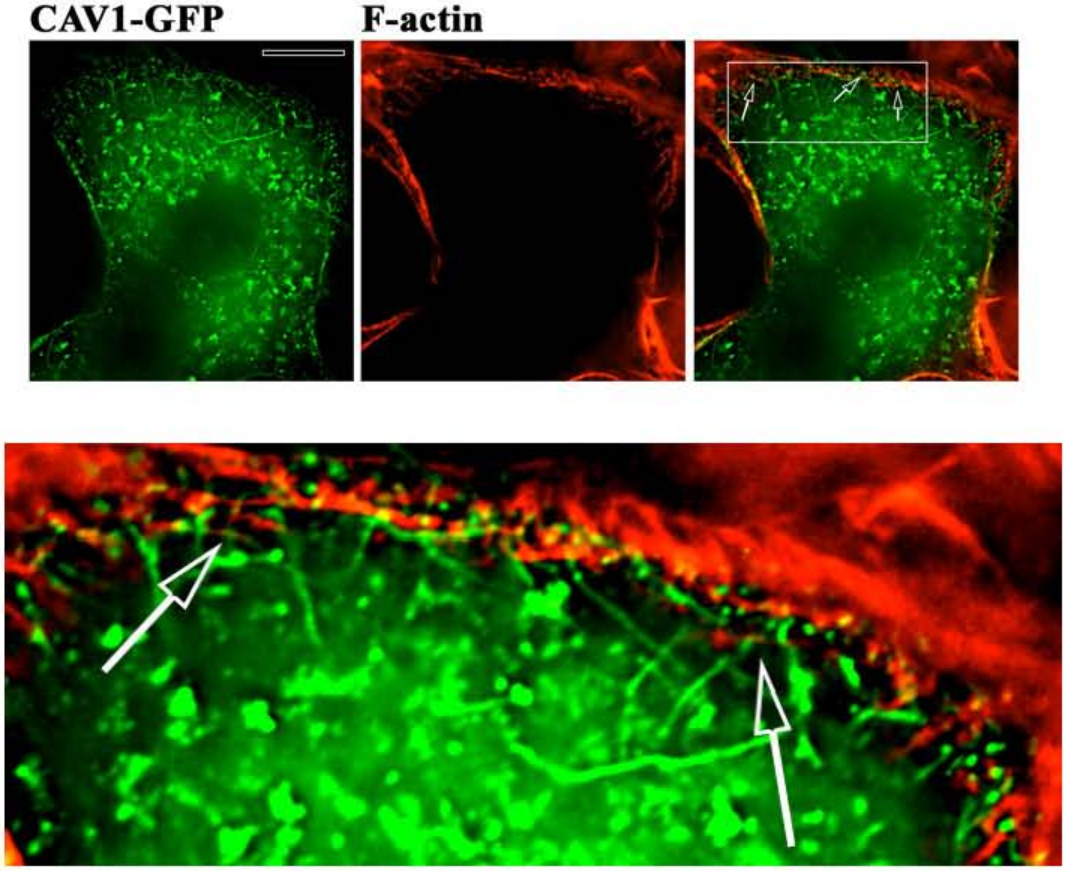
CAV1-GFP
F-actin

Figure 32. Long tubules of caveolin-1 are closely associated with the cortical actin cytoskeleton. SKBr3 cells were transiently transfected with caveolin-1-GFP and Ds-red-actin, fix, permeabilized and visualized through epifluorescence microscope. The image on the right is the merged image. The boxed area is enlarged in the bottom panel with arrows pointing at the close association of actin and caveolin-1-GFP. Scale bar (applies to all panels); 5 μm.

Protein	Treatment	% Decrease in Long Tubule Length, 10 minutes
Caveolin-1-GFP	**Control**	**68.5 ± 14.64, n=8**
Caveolin-1-GFP	**Latrunculin A**	**15.4 ± 10.11, n=5**
Caveolin-1-RFP	**Control**	**67.2 ± 14.23, n=5**
Caveolin-1-RFP	**Blebbistatin**	**10 ± 4.79, n=5**

Table 1. Effect of latrunculin A and blebbistatin on caveolin-1 tubule stability. Total tubule length in SKBr3 cells expressing caveolin-1-GFP or caveolin-1-RFP (drug-treated as indicated) was measured in one frame of a live-cell time-lapse movie, and in a second frame 10 minutes later. Average percent decrease in tubule length in that time is shown. As blebbistatin is toxic to cells expressing GFP (Kolega, 2004), caveolin-1-RFP was used for those experiments. The "n" represents the number of cells used in the calculations.

Chapter 5. Discussion

Part I ErbB2 internalization and trafficking induced by caveolin-1 expression.

Our hypothesis was that over-expression of caveolin-1 caused the downregulation of ErbB2 receptor via the caveolar pathway in SKBr3 cells. Our initial immunofluorescence experiments suggested that exogenous expression of caveolin-1 alone in SKBr3 cells resulted in a reduction of ErbB2 levels at the cell surface and enhanced internalization. This observation seemed to point to an important possible role for caveolin-1 as a negative regulator of ErbB2. We were intrigued by the possible that caveolin-1 modulated ErbB2 receptor levels by promoting internalization and degradation. This might help explain how the protein acted as a tumor suppressor in ErbB2-overexpressing cells, and why it was lost in cancer.

However, further experiments did not support these initial observations. We were unable to reproducibly demonstrate an effect of caveolin-1 expression on ErbB2 localization or internalization rate. We concluded that initial observations were based on overly-optimistic interpretations of immunofluorescence images of a few rare individual cells that were not representative of most cells in the population.

Furthermore, we were initially misled by internal organelles that were highly enriched in both ErbB2 and caveolin-1 (Fig. 9). We initially concluded

that these represented caveosomes, or other novel endocytic structures dedicated to internalization of ErbB2 together with caveolin-1. However, further work showed that these were in fact early endosomes, and contained early endosome markers as well cargo internalized by the clathrin-dependent pathway as well as ErbB2 and caveolin-1.

Recent work from my lab showed that ErbB2 was internalized by a non-clathrin mechanism that probably corresponds to bulk-phase endocytosis, with or without GA treatment or caveolin-1 expression. After internalization, ErbB2 is rapidly transported to early endosome and then late endosome by the classical endocytic transport pathway (Barr *et al.*, 2008). Because we found no evidence for a specific involvement of caveolin-1 with ErbB2 trafficking, we did not pursue this project further.

Part II Interaction with actomyosin exerts tension on membrane tubules induced by caveolin-1 expression in breast cancer cells

We found that caveolin-1-GFP expressed in SKBr3 cells was present in membrane tubules much more frequently than when expressed in normal cells. As internalized CTxB was rarely present on tubules in untransfected cells, but efficiently labeled tubules in caveolin-1-GFP-transfected cells, we concluded that caveolin-1-GFP induced tubule formation.

Live cell imaging enabled us to look at caveolin-1-GFP tubular dynamics in more detail. We found that caveolin-1-GFP tubules were very dynamic and showed elongation and retraction. However, we never saw tubules being formed. We speculate that this was because tubule formation was a rare event. Tubules were only seen in about 15% of transfected cells at steady state. We attempted to do live cell imaging of individual transfected cells that did not show tubules, hoping to observe tubule formation over time. Unfortunately, because of fairly rapid GFP bleaching, and the fact that we could focus on only one cell at a time with 100x oil immersion objective, we did not succeed in observing new tubules forming.

The frequency of tubular localization of transfected caveolin-1-GFP correlated inversely with the level of endogenous caveolin-1 expression in several cell lines. Expression of caveolin-1 in normal cells that lack the protein is sufficient for formation of invaginated caveolae (Fra *et al.*, 1995), though recent studies have shown that PTRF/cavin is also required (Hill *et al.*, 2008; Liu *et al.*, 2008). Together, these findings suggest that caveolin-1 contributes to membrane deformation and induction of curvature. Caveolin proteins have an unusual topology: N- and C-terminal hydrophilic domains on the cytosolic side of the membrane flank a central hydrophobic domain that is membrane-associated, and is presumed to form a hydrophobic hairpin in the membrane (Fig. 2) (Parton and Simons, 2007).

Reticulons, among the few proteins to share this topology, deform the endoplasmic reticulum into tubules (Hu *et al.*, 2008), possibly by inserting preferentially into the cytosolic leaflet of the bilayer and inducing curvature via a bilayer-coupling mechanism. Thus, caveolins might deform membranes by the same mechanism (Fig. 33).

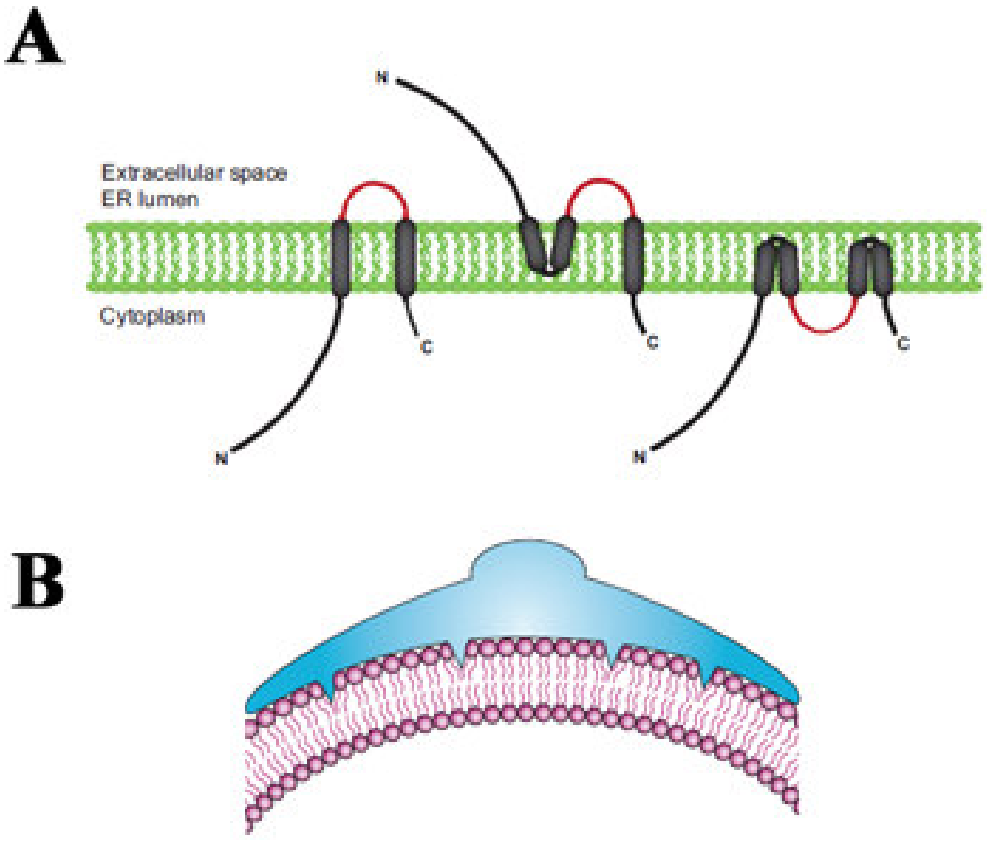

Figure 33. How membrane proteins can generate curvature in membrane? (taken from (Yang and Strittmatter, 2007)) (A) Shows the possible topologies of reticulon proteins in membranes. These three different topologies have been shown to exist. Depending up on cell type and membrane, reticulon proteins may adapt a certain topology. (B) A model of how caveolin-1 can induced curvature in membranes. Caveolin-1 has an amphipathic domain which can be inserted between the polar headgroups of lipid molecules.

In most cells, caveolin-1 induces formation of caveolae, which can exist in clusters in cells where they are abundant. We found that membrane tubules induced by caveolin-1 in breast cancer cells are derived from the plasma membrane, remain closely-associated with the plasma membrane, and retain plasma membrane characteristics. We speculate that tubules represent exaggerated versions of normal caveolae. The same properties of caveolin-1 that normally result in caveolae formation induce further membrane deformation and tubule formation in breast cancer cells. This model suggests that normal cells have mechanisms to limit caveolin-induced membrane deformation and largely prevent tubule formation. This could explain why caveolin-1-positive tubules have occasionally been observed previously, but are rare. Our results suggest that normal mechanisms for limiting tubule formation operate less efficiently in transformed cells. An analogy to dynamin proteins helps illustrate this model. Dynamins can deform membranes and induce tubule formation in model membranes. By contrast, in cells, dynamins act late in clathrin-coated vesicle formation, in the scission step. Only when the GTPase activity of dynamin is inhibited do abnormal dynamin-induced tubules form. (Dynamins also act in caveolar endocytosis, and it might be imagined that abnormal dynamin function in breast cancer cells contributed to the caveolin-1- positive tubules that we observed. This seems unlikely, as dynamin-dependent clathrin-mediated

endocytosis occurs normally in these cells (Barr *et al.*, 2008a)). We found no evidence for a function for caveolin-1 tubules, and no evidence that they delivered endocytic cargo to endosomes. We speculate that they may be aberrant, dead-end structures. We found that caveolin-1 tubules were unstable, and broke down rapidly. After breakage, tubules sometimes resolved into motile caveolin-1-positive vesicles that resembled those described in normal cells (Mundy *et al.*, 2002). Nevertheless, tubule formation might be detrimental to cells, and might exert selective pressure on cancer cells to lose caveolin-1 expression. A tubular localization of EHD proteins and Rab8 has been previously reported (Roland *et al.*, 2007a), and these proteins are present on the same tubules when co-expressed in HeLa cells. These tubules have many properties in common with the caveolin-1-GFP tubules we observed. Both are microtubule-dependent and regulated by Arf6. Furthermore, actin filament depolymerization greatly increased the frequency of cells exhibiting Rab8-positive tubules, just as we found for caveolin-1-induced tubules. As is true for caveolin-1, no clear function for Rab8 or EHD-positive tubules has been demonstrated. It's difficult to test for a specific function for tubule-localized EHD proteins, as the proteins localize both to tubules and to punctate structures. Nevertheless, in a structural study of EHD2, McMahon and colleagues showed that the protein favored binding to curved membranes in vitro, and induced tubule formation (Daumke *et al.*, 2007). They speculated that tubules induced by EHD proteins might be induced through over-expression rather than

performing a normal physiological function. Proteins that bind preferentially to curved membranes stabilize curvature upon binding, blurring the distinction between proteins that favor binding to curved membranes and proteins that induce curvature in fluctuating membranes. Thus, EHD proteins and Rab8 might be present on caveolin-1-positive tubules in SKBr3 cells simply because they favor binding to membranes with that degree of curvature. Alternatively, the three proteins might work together in a process such as membrane recycling, as EHD proteins act in this function. From a mechanistic viewpoint, the ability of caveolin-1 and Rab8-Q67L to synergize in tubule formation is intriguing. It is not known how Rab8 promotes tubule formation, but this finding suggests it works through a different and complementary mechanism than caveolin-1. Depolymerization of actin filaments with latrunculin stabilized the tubules. This probably contributed to the increased frequency of cells containing caveolin-1-GFP-positive tubules after latrunculin treatment. We do not know whether actin depolymerization also enhanced tubule formation, through a separate mechanism. A network of actin filaments linked to myosin II underlies the plasma membrane of mammalian cells and forms the actomyosin subcortical cytoskeleton. The unique structure of myosin II allows it to induce tension on actin filaments (Clark *et al.*, 2007). Myosin II consists of a head, containing the actin-binding motor, and an elongated coiled coil domain. Myosin II monomers oligomerize via their coiled-coil domains to form bipolar filaments, containing monomers oriented in

opposite directions. Binding of oppositely-oriented myosin II heads to different actin filaments pulls the actin filaments together when the myosin II motor is activated, inducing tension (Clark *et al.*, 2007). Myosin II activity is highly regulated through phosphorylation of its light chain by myosin light chain kinase (MLCK) and by ROCK. RhoA regulates myosin II activity indirectly, by activating ROCK. This cortical contractility can aid in retraction of the cell body during migration, and cleavage furrow ingression during cell division (Paluch *et al.*, 2006).

Caveolae are linked to the actin cytoskeleton (Pelkmans *et al.*, 2002; Thomsen *et al.*, 2002), but the function of this linkage is not known. We found that linkage of caveolin-1 tubules to actomyosin induces enough tension on the membranes to break the tubules. As caveolae in normal cells are likely to interact with the actin cytoskeleton by the same mechanism, they could also be under tension. If tension were counteracted in normal cells by mechanisms that prevented further deformation of caveolae into tubules, the tension would be hard to detect, explaining why it has not been appreciated to date. However, such tension might play a role in the function of caveolin-1 in processes that depend on the actin cytoskeleton. At least two such functions of caveolin-1 have been described: mechanosensation (Parton and Simons, 2007) and directional cell migration (Grande-García *et al.*, 2007; Sun *et al.*, 2007). Although it is not yet clear how cortical tension affect function of caveolin-1, at least two possibilities

can be imagined. First, mechanical force can stretch actin-binding proteins, changing their conformation and exposing cryptic binding sites. For instance, binding sites for vinculin are exposed upon stretching of talin (Vogel and Sheetz, 2009).

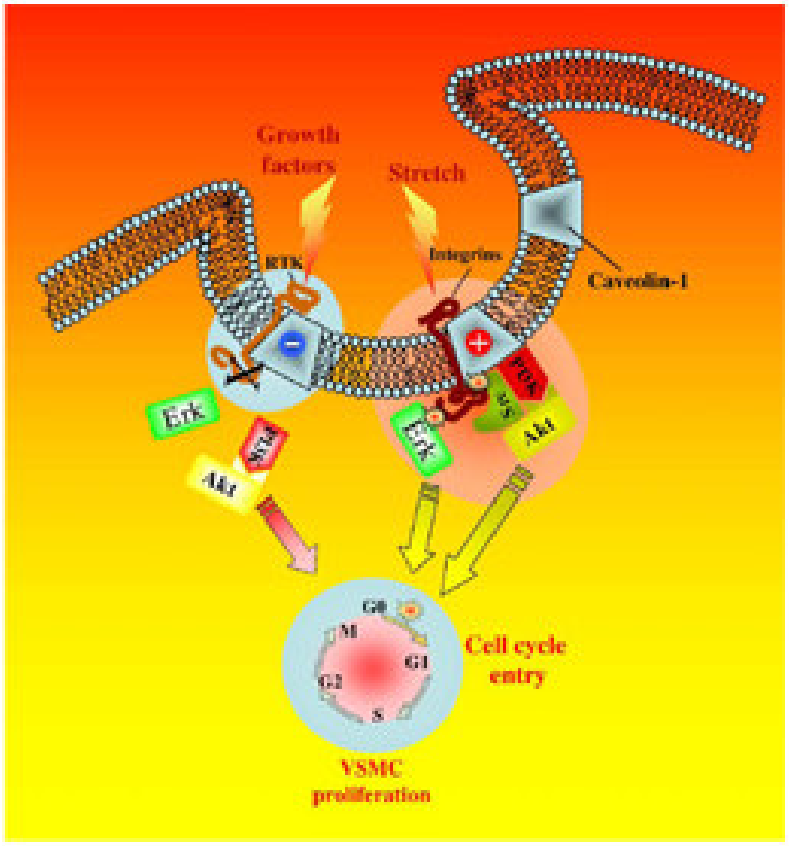

Figure 34. Dual role of caveolin-1 in proliferation of vascular smooth muscles cells (VSMC) (taken from (Sedding and Braun-Dullaeus, 2006)). The diagram shows how on one hand caveolin-1 can retard cell growth triggered by receptor tyrosine kinase (RTK). On the other hand, in response to mechanical stress and strain, it positively induces the cell cycle entry and progression of VSMC.

Stretching of caveolin-1 or another caveolar protein that was bound to actomyosin might have a similar effect. As one possibility, stretching of caveolin-1 might affect the caveolin-1-scaffolding domain (CSD), a domain of caveolin-1 just upstream from the hydrophobic domain. Puzzlingly, although this domain has been reported to bind to and regulate a number of signaling proteins (Fig. 34) (Williams and Lisanti, 2005), model membrane studies have shown that it lies flat on the membrane surface (Arbuzova *et al.*, 2000), presumably limiting its ability to bind other proteins. Actomyosin-induced stretching of caveolin-1 could pull the CSD off the membrane, facilitating interaction with its binding partners. A second possibility, suggested earlier (Parton and Simons, 2007), is that mechanical force could affect the membrane elasticity of the raft-like caveolar membrane, thereby affecting the function of caveolar proteins by changing the physical properties of the surrounding bilayer. By this mechanism, local changes in actomyosin-induced tension on the caveolar membrane might differentially affect the function of caveolar proteins in different parts of the cell surface.

Caveolae and signalling molecules

SKBr3 human breast cancer cells do not express caveolin-1. This suggests that caveolin-1 may be acting as a tumor suppressor protein. The function of caveolin-1 is to act as a scaffolding proteins to organize and concentrate specific

lipids (cholesterol and glycosphingolipids) and lipid-modified signaling molecules (Src-like kinases, H-Ras, endothelial NOS) within caveolae. The caveolin-1 scaffolding domain (CSD) of caveolin-1 binds to different receptor molecules and prevents them from signaling. Epidermal growth factor (EGF) receptor, platelet-derived growth factor (PDGF) receptor, transforming growth factor-β receptor and neurotrophin receptors are the few examples of receptors that are down-regulated by caveolin-1 (Bilderback *et al.*, 1999; Yamamoto *et al.*, 1999; Razani *et al.*, 2001). One hypothesis is that caveolin-1 acts as storage for different signalling molecules keeping them under restrain. Caveolin-1 creates a launching platform for all the downstream growth pathways. The check is released under specific circumstance. But this hypothesis needs to be tested. This could explain why caveolin-1 is downregulated in many types of primary tumors. On the other hand elevated levels of caveolin-1 promote resistance to apoptosis and chemotherapeutic drugs allowing the development of increased cellular survival, invasiveness, motility and multidrug resistance. The highly complex relationship between caveolin-1 and tumor progression clearly underscores the role of caveolin-1 in variety of cellular functions as well as its multiple interactions with the signalling proteins that shape tumor cell behavior.

Conclusions, models, and further directions

The major finding of this project was that caveolin-1 induces formation of cytoskeleton-dependent membrane tubules more frequently in breast cancer cells than in normal cells. In addition, characterization of the tubules gave us insights into their dynamics that probably also apply to caveolae in normal cells. Caveolin-1 has been reported to be involved in interaction with actin and microtubule cytoskeleton in normal cells. The mechanism is relatively unknown. Caveolin-1 has also been shown to function of actin-related processes like mechanotransduction and directional cell motility. However, nothing is known about how this might occur. We found for the first time that in addition to binding to actin filaments, caveolin-1 tubules are under tension, induced by interaction with the actomyosin cytoskeleton. This finding suggests that this tension might aid in caveolin-1 function in actin-dependent processes. In the future, it will be interesting to test this model further by further characterizing the interaction between caveolae and the actin cytoskeleton, by identifying the proteins involved. This will allow us to determine whether these links are required for caveolin-1 function. Caveolin-1 membrane tubules should be a great tool to gain more insights into the role of caveolin-1 in actomyosin tension.

Bibliography

Ang, A.L., Fölsch, H., Koivisto, U.M., Pypaert, M., and Mellman, I. (2003). The Rab8 GTPase selectively regulates AP-1B–dependent basolateral transport in polarized Madin-Darby canine kidney cells. J. Cell Biol. *163*, 339-350.

Austin, C.D., De Maziere, A.M., Pisacane, P.I., van Dijk, S.M., Eigenbrot, C., Sliwkowski, M.X., Klumperman, J., and Scheller, R.H. (2004). Endocytosis and sorting of ErbB2 and the site of action of cancer therapeutics trastuzumab and geldanamycin. Mol Biol Cell *15*, 5268-5282.

Bao, J., Jana, S.S., and Adelstein, R.S. (2005). Vertebrate nonmuscle myosin II isoforms rescue small interfering RNA-induced defects in COS-7 cell cytokinesis. J Biol Chem *280*, 19594-19599.

Barr, D.J., Ostermeyer-Fay, A.G., Matundan, R.A., and Brown, D.A. (2008). Clathrin-independent endocytosis of ErbB2 in geldanamycin-treated human breast cancer cells. J Cell Sci *121*, 3155-3166.

Bilderback, T.R., Gazula, V.R., Lisanti, M.P., and Dobrowsky, R.T. (1999). Caveolin interacts with Trk A and p75(NTR) and regulates neurotrophin signaling pathways. J Biol Chem *274*, 257-263.

Blume, J.J., Halbach, A., Behrendt, D., Paulsson, M., and Plomann, M. (2007). EHD proteins are associated with tubular and vesicular compartments and interact with specific phospholipids. Exp Cell Res *313*, 219-231.

Braun, A., Pinyol, R., Dahlhaus, R., Koch, D., Fonarev, P., Grant, B.D., Kessels, M.M., and Qualmann, B. (2005). EHD proteins associate with syndapin I and II and such interactions play a crucial role in endosomal recycling. Mol Biol Cell *16*, 3642-3658.

Brown, S.S. (1999). Cooperation between microtubule- and actin-based motor proteins. Annu Rev Cell Dev Biol *15*, 63-80.

Caplan, S., Naslavsky, N., Hartnell, L.M., Lodge, R., Polishchuk, R.S., Donaldson, J.G., and Bonifacino, J.S. (2002). A tubular EHD1-containing compartment involved in the recycling of major histocompatibility complex class I molecules to the plasma membrane. Embo J *21*, 2557-2567.

Capozza, F., Williams, T.M., Schubert, W., McClain, S., Bouzahzah, B., Sotgia, F., and Lisanti, M.P. (2003). Absence of caveolin-1 sensitizes mouse skin to

carcinogen-induced epidermal hyperplasia and tumor formation. Am J Pathol *162*, 2029-2039.

Clark, K., Langeslag, M., Figdor, C.G., and van Leeuwen, F.N. (2007). Myosin II and mechanotransduction: a balancing act. Trends Cell Biol *17*, 178-186.

Cremona, O., al, e., and de Camilli, P. (1999). Essential role of phosphoinositide metabolism in synaptic vesicle recycling. Cell *99*, 179-188.

Daumke, O., Lundmark, R., Vallis, Y., Martens, S., Butler, P.J., and McMahon, H.T. (2007). Architectural and mechanistic insights into an EHD ATPase involved in membrane remodelling. Nature *449*, 923-927.

del Toro, D., Jordi Alberch, F.L.-D., Raquel Martín-Ibáñez, Xavier Xifró, Gustavo Egea, and Josep M. , and Canals, J.M. (2009). Mutant Huntingtin Impairs Post-Golgi Trafficking to Lysosomes by Delocalizing Optineurin/Rab8 Complex from the Golgi Apparatus. Mol. Biol. Cell *20*, 1478-1492.

Denker, S.P., McCaffrey, J.M., Palade, G.E., Insel, P.A., and Farquhar, M.G. (1996). Differential distribution of α subunits and βγ subunits of heterotrimeric G proteins on Golgi membranes of the exocrine pancreas. J. Cell Biol. *133*, 1027-1040.

Devreotes, P., and Janetopoulos, C. (2003). Eukaryotic chemotaxis: distinctions between directional sensing and polarization. J Biol Chem *278*, 20445-20448.

Echarri, A., Muriel, O., and Del Pozo, M.A. (2007). Intracellular trafficking of raft/caveolae domains: insights from integrin signaling. Semin Cell Dev Biol *18*, 627-637.

Endow, S.A. (2003). Kinesin motors as molecular machines. Bioessays *25*, 1212-1219.

Engelman, J.A., Wykoff, C.C., Yasuhara, S., Song, K.S., Okamoto, T., and Lisanti, M.P. (1997). Recombinant expression of caveolin-1 in oncogenically transformed cells abrogates anchorage-independent growth. J Biol Chem *272*, 16374-16381.

Engelman, J.A., Zhang, X.L., Galbiati, F., and Lisanti, M.P. (1998). Chromosomal localization, genomic organization, and developmental expression of the murine caveolin gene family (Cav-1, -2, and -3). Cav-1 and Cav-2 genes map to a known tumor suppressor locus (6-A2/7q31). FEBS Lett *429*, 330-336.

Frank, S.R., Hatfield, J.C., and Casanova, J.E. (1998). Remodeling of the actin cytoskeleton is coordinately regulated by protein kinase C and the ADP-ribosylation factor nucleotide exchange factor ARNO. Mol. Biol. Cell *9*, 3133-3146.

Fuchs, E., and Yang, Y. (1999). Crossroads on cytoskeletal highways. Cell *98*, 547-550.

Galbiati, F., Volonte, D., Engelman, J.A., Watanabe, G., Burk, R., Pestell, R.G., and Lisanti, M.P. (1998). Targeted downregulation of caveolin-1 is sufficient to drive cell transformation and hyperactivate the p42/44 MAP kinase cascade. EMBO J *17*, 6633-6648.

Galperin, E., Benjamin, S., Rapaport, D., Rotem-Yehudar, R., Tolchinsky, S., and Horowitz, M. (2002). EHD3: a protein that resides in recycling tubular and vesicular membrane structures and interacts with EHD1. Traffic *3*, 575-589.

Garcia-Cardena, G., Martasek, P., Masters, B.S., Skidd, P.M., Couet, J., Li, S., Lisanti, M.P., and Sessa, W.C. (1997). Dissecting the interaction between nitric oxide synthase (NOS) and caveolin. Functional significance of the nos caveolin binding domain in vivo. J Biol Chem *272*, 25437-25440.

George, M., Ying, G., Rainey, M.A., Solomon, A., Parikh, P.T., Gao, Q., Band, V., and Band, H. (2007). Shared as well as distinct roles of EHD proteins revealed by biochemical and functional comparisons in mammalian cells and C. elegans. BMC Cell Biol *8*, 3.

Goetz, J.G., Lajoie, P., Wiseman, S.M., and Nabi, I.R. (2008). Caveolin-1 in tumor progression: the good, the bad and the ugly. Cancer Metastasis Rev *27*, 715-735.

Golomb, E., Ma, X., Jana, S.S., Preston, Y.A., Kawamoto, S., Shoham, N.G., Goldin, E., Conti, M.A., Sellers, J.R., and Adelstein, R.S. (2004). Identification and characterization of nonmuscle myosin II-C, a new member of the myosin II family. J Biol Chem *279*, 2800-2808.

Grande-Garcia, A., and del Pozo, M.A. (2008). Caveolin-1 in cell polarization and directional migration. Eur J Cell Biol *87*, 641-647.

Grant, B., Zhang, Y., Paupard, M.C., Lin, S.X., Hall, D.H., and Hirsh, D. (2001). Evidence that RME-1, a conserved C. elegans EH-domain protein, functions in endocytic recycling. Nat Cell Biol *3*, 573-579.

Guilherme, A., Soriano, N.A., Bose, S., Holik, J., Bose, A., Pomerleau, D.P., Furcinitti, P., Leszyk, J., Corvera, S., and Czech, M.P. (2004a). EHD2 and the novel EH domain binding protein EHBP1 couple endocytosis to the actin cytoskeleton. J Biol Chem *279*, 10593-10605.

Guilherme, A., Soriano, N.A., Furcinitti, P.S., and Czech, M.P. (2004b). Role of EHD1 and EHBP1 in perinuclear sorting and insulin-regulated GLUT4 recycling in 3T3-L1 adipocytes. J Biol Chem *279*, 40062-40075.

Hailstones, D., Sleer, L.S., Parton, R.G., and Stanley, K.K. (1998). Regulation of caveolin and caveolae by cholesterol in MDCK cells. J. Lipid. Res. *39*, 369-379.

Hattula, K., Furuhjelm, J., Tikkanen, J., Tanhuanpaa, K., Laakkonen, P., and Peranen, J. (2006). Characterization of the Rab8-specific membrane traffic route linked to protrusion formation. J Cell Sci *119*, 4866-4877.

Hayashi, K., Matsuda, S., Machida, K., Yamamoto, T., Fukuda, Y., Nimura, Y., Hayakawa, T., and Hamaguchi, M. (2001). Invasion activating caveolin-1 mutation in human scirrhous breast cancers. Cancer Res *61*, 2361-2364.

Hernández-Deviez, D.J., Roth, M.G., Casanova, J.E., and Wilson, J.M. (2004). ARNO and ARF6 regulate axonal elongation and branching through downstream activation of phosphatidylinositol 4-phosphate 5-kinase alpha. Mol. Biol. Cell *15*, 111-120.

Hodge, T., and Cope, M.J. (2000). A myosin family tree. J Cell Sci *113 Pt 19*, 3353-3354.

Hommelgaard, A.M., Lerdrup, M., and van Deurs, B. (2004). Association with membrane protrusions makes ErbB2 an internalization-resistant receptor. Mol Biol Cell *15*, 1557-1567.

Huber, L.A., Pimplikar, S., Parton, R.G., Vira, H., Zerial, M., and Simons, K. (1993). Rab8, a small GTPase involved in vesicular traffic between the TGN and the basolateral membrane. J. Cell Biol. *123*, 35-45.

Iwahashi, J., Kawasaki, I., Kohara, Y., Gengyo-Ando, K., Mitani, S., Ohshima, Y., Hamada, N., Hara, K., Kashiwagi, T., and Toyoda, T. (2002). Caenorhabditis elegans reticulon interacts with RME-1 during embryogenesis. Biochem Biophys Res Commun *293*, 698-704.

Joo, H.J., Oh, D.K., Kim, Y.S., Lee, K.B., and Kim, S.J. (2004). Increased expression of caveolin-1 and microvessel density correlates with metastasis and poor prognosis in clear cell renal cell carcinoma. BJU Int *93*, 291-296.

Kalia, M., Kumari, S., Chadda, R., Hill, M.M., Parton, R.G., and Mayor, S. (2006). Arf6-independent GPI-anchored protein-enriched early endosomal compartments fuse with sorting endosomes via a Rab5/phosphatidylinositol-3'-kinase–dependent machinery. Mol. Biol. Cell *17*, 3689-3704.

Kato, K., Hida, Y., Miyamoto, M., Hashida, H., Shinohara, T., Itoh, T., Okushiba, S., Kondo, S., and Katoh, H. (2002). Overexpression of caveolin-1 in esophageal squamous cell carcinoma correlates with lymph node metastasis and pathologic stage. Cancer *94*, 929-933.

Kolega, J. (2004). Phototoxicity and photoinactivation of blebbistatin in UV and visible light. Biochem. Biophys. Res. Commun.. *320*, 1020-1025.

Kolega, J. (2006). The role of myosin II motor activity in distributing myosin asymmetrically and coupling protrusive activity to cell translocation. Mol Biol Cell *17*, 4435-4445.

Koleske, A.J., Baltimore, D., and Lisanti, M.P. (1995). Reduction of caveolin and caveolae in oncogenically transformed cells. Proc Natl Acad Sci U S A *92*, 1381-1385.

Krendel, M., and Mooseker, M.S. (2005). Myosins: tails (and heads) of functional diversity. Physiology (Bethesda) *20*, 239-251.

Lapierre, L.A., Kumar, R., Hales, C.M., Navarre, J., Bhartur, S.G., Burnette, J.O., Provance, D.W.J., Mercer, J.A., Bähler, M., and Goldenring, J.R. (2001). Myosin Vb is associated with plasma membrane recycling systems. Mol. Biol. Cell *12*, 1843-1857.

Lencer, W.I., and Tsai, B. (2003). The intracellular voyage of cholera toxin: going retro. Trends Biochem Sci *28*, 639-645.

Li, R., and Gundersen, G.G. (2008). Beyond polymer polarity: how the cytoskeleton builds a polarized cell. Nat Rev Mol Cell Biol *9*, 860-873.

Li, S., Couet, J., and Lisanti, M.P. (1996). Src tyrosine kinases, Galpha subunits, and H-Ras share a common membrane-anchored scaffolding protein, caveolin. Caveolin binding negatively regulates the auto-activation of Src tyrosine kinases. J Biol Chem *271*, 29182-29190.

Li, S., Okamoto, T., Chun, M., Sargiacomo, M., Casanova, J.E., Hansen, S.H., Nishimoto, I., and Lisanti, M.P. (1995). Evidence for a regulated interaction between heterotrimeric G proteins and caveolin. J Biol Chem *270*, 15693-15701.

Linder, M.D., Uronen, R.-L., Hölttä-Vuori, M., van der Sluijs, P., Peränen, J., and Ikonen, E. (2007). Rab8-dependent recycling promotes endosomal cholesterol removal in normal and sphingolipidosis cells. Mol. Biol. Cell *18*, 47-56.

Lippincott-Schwartz, J., al, e., and Klausner, R.D. (1991). Forskolin inhibits and reverses the effects of brefeldin A on Golgi morphology by a cAMP-independent mechanism. J. Cell Biol. *112*, 567-577.

Mallik, R., and Gross, S.P. (2004). Molecular motors: strategies to get along. Curr Biol *14*, R971-982.

Mintz, L., Galperin, E., Pasmanik-Chor, M., Tulzinsky, S., Bromberg, Y., Kozak, C.A., Joyner, A., Fein, A., and Horowitz, M. (1999). EHD1--an EH-domain-containing protein with a specific expression pattern. Genomics *59*, 66-76.

Monier, S., Parton, R.G., Vogel, F., Behlke, J., Henske, A., and Kurzchalia, T.V. (1995). VIP21-caveolin, a membrane protein constituent of the caveolar coat, oligomerizes in vivo and in vitro. Mol Biol Cell *6*, 911-927.

Montesano, R., Roth, J., Robert, A., and Orci, L. (1982). Non-coated membrane invaginations are involved in binding and internalization of cholera and tetanus toxins. Nature *296*, 651-653.

Mundy, D.I., Machleidt, T., Ying, Y.S., Anderson, R.G., and Bloom, G.S. (2002). Dual control of caveolar membrane traffic by microtubules and the actin cytoskeleton. J Cell Sci *115*, 4327-4339.

Munro, P., Kojima, H., Dupont, J.L., Bossu, J.L., Poulain, B., and Boquet, P. (2001). High sensitivity of mouse neuronal cells to tetanus toxin requires a GPI-anchored protein. Biochem Biophys Res Commun *289*, 623-629.

Naslavsky, N., Boehm, M., Backlund, P.S., Jr., and Caplan, S. (2004a). Rabenosyn-5 and EHD1 interact and sequentially regulate protein recycling to the plasma membrane. Mol Biol Cell *15*, 2410-2422.

Naslavsky, N., and Caplan, S. (2005). C-terminal EH-domain-containing proteins: consensus for a role in endocytic trafficking, EH? J. Cell Sci. *118*, 4093-4101.

Naslavsky, N., McKenzie, J., Altan-Bonnet, N., Sheff, D., and Caplan, S. (2009). EHD3 regulates early-endosome-to-Golgi transport and preserves Golgi morphology. J Cell Sci *122*, 389-400.

Naslavsky, N., Rahajeng, J., Sharma, M., Jovic, M., and Caplan, S. (2006). Interactions between EHD proteins and Rab11-FIP2: a role for EHD3 in early endosomal transport. Mol Biol Cell *17*, 163-177.

Naslavsky, N., Weigert, R., and Donaldson, J.G. (2003). Convergence of non-clathrin- and clathrin-derived endosomes involves Arf6 inactivation and changes in phosphoinositides. Mol Biol Cell *14*, 417-431.

Naslavsky, N., Weigert, R., and Donaldson, J.G. (2004b). Characterization of a nonclathrin endocytic pathway: membrane cargo and lipid requirements. Mol Biol Cell *15*, 3542-3552.

Nichols, B. (2003). Caveosomes and endocytosis of lipid rafts. J Cell Sci *116*, 4707-4714.

Ostermeyer, A.G., Paci, J.M., Zeng, Y., Lublin, D.M., Munro, S., and Brown, D.A. (2001). Accumulation of caveolin in the endoplasmic reticulum redirects the protein to lipid storage droplets. J Cell Biol *152*, 1071-1078.

Ostermeyer, A.G., Ramcharan, L.T., Zeng, Y., Lublin, D.M., and Brown, D.A. (2004). Role of the hydrophobic domain in targeting caveolin-1 to lipid droplets. J. Cell Biol. *164*, 69-78.

Ostrom, R.S., and Insel, P.A. (2004). The evolving role of lipid rafts and caveolae in G protein-coupled receptor signaling: implications for molecular pharmacology. Br J Pharmacol *143*, 235-245.

Park, S.Y., Ha, B.G., Choi, G.H., Ryu, J., Kim, B., Jung, C.Y., and Lee, W. (2004). EHD2 interacts with the insulin-responsive glucose transporter (GLUT4) in rat adipocytes and may participate in insulin-induced GLUT4 recruitment. Biochemistry *43*, 7552-7562.

Parton, R.G., Joggerst, B., and Simons, K. (1994). Regulated internalization of caveolae. J Cell Biol *127*, 1199-1215.

Parton, R.G., and Richards, A.A. (2003). Lipid rafts and caveolae as portals for endocytosis: new insights and common mechanisms. Traffic *4*, 724-738.

Parton, R.G., and Simons, K. (2007). The multiple faces of caveolae. Nat Rev Mol Cell Biol *8*, 185-194.

Pelkmans, L., Burli, T., Zerial, M., and Helenius, A. (2004). Caveolin-stabilized membrane domains as multifunctional transport and sorting devices in endocytic membrane traffic. Cell *118*, 767-780.

Pelkmans, L., Kartenbeck, J., and Helenius, A. (2001). Caveolar endocytosis of simian virus 40 reveals a new two-step vesicular-transport pathway to the ER. Nat Cell Biol *3*, 473-483.

Pelkmans, L., Puntener, D., and Helenius, A. (2002). Local actin polymerization and dynamin recruitment in SV40-induced internalization of caveolae. Science *296*, 535-539.

Peränen, J., Auvinen, P., Virta, H., Wepf, R., and Simons, K. (1996). Rab8 promotes polarized membrane transport through reorganization of actin and microtubules in fibroblasts. J. Cell Biol. *135*, 153-167.

Peters, P.J., Mironov, A., Jr., Peretz, D., van Donselaar, E., Leclerc, E., Erpel, S., DeArmond, S.J., Burton, D.R., Williamson, R.A., Vey, M., and Prusiner, S.B. (2003). Trafficking of prion proteins through a caveolae-mediated endosomal pathway. J Cell Biol *162*, 703-717.

Pohl, U., Smith, J.S., Tachibana, I., Ueki, K., Lee, H.K., Ramaswamy, S., Wu, Q., Mohrenweiser, H.W., Jenkins, R.B., and Louis, D.N. (2000). EHD2, EHD3, and EHD4 encode novel members of a highly conserved family of EH domain-containing proteins. Genomics *63*, 255-262.

Pollard, T.D., and Borisy, G.G. (2003). Cellular motility driven by assembly and disassembly of actin filaments. Cell *112*, 453-465.

Provance, D.W., Jr., Addison, E.J., Wood, P.R., Chen, D.Z., Silan, C.M., and Mercer, J.A. (2008). Myosin-Vb functions as a dynamic tether for peripheral endocytic compartments during transferrin trafficking. BMC Cell Biol *9*, 44.

Quest, A.F., Gutierrez-Pajares, J.L., and Torres, V.A. (2008). Caveolin-1: an ambiguous partner in cell signalling and cancer. J Cell Mol Med *12*, 1130-1150.

Razani, B., Zhang, X.L., Bitzer, M., von Gersdorff, G., Bottinger, E.P., and Lisanti, M.P. (2001). Caveolin-1 regulates transforming growth factor (TGF)-beta/SMAD signaling through an interaction with the TGF-beta type I receptor. J Biol Chem *276*, 6727-6738.

Ren, X., Ostermeyer, A.G., Ramcharan, L.T., Zeng, Y., Lublin, D.M., and Brown, D.A. (2004). Conformational defects slow Golgi exit, block oligomerization, and reduce raft affinity of caveolin-1 mutant proteins. Mol. Biol. Cell *15*, 4556-4567.

Rodriguez, O.C., and Cheney, R.E. (2002). Human myosin-Vc is a novel class V myosin expressed in epithelial cells. J. Cell Sci. *115*, 991–1004.

Roland, J.T., Kenworthy, A.K., Peranen, J., Caplan, S., and Goldenring, J.R. (2007a). Myosin Vb interacts with Rab8a on a tubular network containing EHD1 and EHD3. Mol Biol Cell *18*, 2828-2837.

Roland, J.T., Kenworthy, A.K., Peranen, J., Caplan, S., and Goldenring, J.R. (2007b). Myosin Vb interacts with Rab8a on a tubular network containing EHD1 and EHD3. Mol. Biol. Cell *18*, 2828-2837.

Ross, J.L., Ali, M.Y., and Warshaw, D.M. (2008). Cargo transport: molecular motors navigate a complex cytoskeleton. Curr Opin Cell Biol *20*, 41-47.

Rotem-Yehudar, R., Galperin, E., and Horowitz, M. (2001). Association of insulin-like growth factor 1 receptor with EHD1 and SNAP29. J Biol Chem *276*, 33054-33060.

Rothberg, K.G., Heuser, J.E., Donzell, W.C., Ying, Y.S., Glenney, J.R., and Anderson, R.G. (1992). Caveolin, a protein component of caveolae membrane coats. Cell *68*, 673-682.

Sahlender, D.A., Roberts, R.C., Arden, S.D., Spudich, G., Taylor, M.J., Luzio, J.P., Kendrick-Jones, J., and Buss, F. (2005). Optineurin links myosin VI to the Golgi complex and is involved in Golgi organization and exocytosis. J. Cell Biol. *169*, 285-295.

Sandquist, J.C., Swenson, K.I., Demali, K.A., Burridge, K., and Means, A.R. (2006). Rho kinase differentially regulates phosphorylation of nonmuscle myosin II isoforms A and B during cell rounding and migration. J Biol Chem *281*, 35873-35883.

Sato, T., Mushiake, S., Kato, Y., Sato, K., Sato, M., Takeda, N., Ozono, K., Miki, K., Kubo, Y., Tsuji, A., Harada, R., and Harada, A. (2007a). The Rab8 GTPase regulates apical protein localization in intestinal cells. Nature *448*, 366-369.

Sato, Y., Shuya Fukai, R.I., and Osamu , and Nureki, O. (2007b). Crystal structure of the Sec4p·Sec2p complex in the nucleotide exchanging intermediate state. Proc. Natl. Acad. Sci U S A *104*, 8305-8310.

Scheiffele, P., Verkade, P., Fra, A.M., Virta, H., Simons, K., and Ikonen, E. (1998). Caveolin-1 and -2 in the exocytic pathway of MDCK cells. J. Cell Biol. *140*, 795-806.

Schlegel, A., Schwab, R.B., Scherer, P.E., and Lisanti, M.P. (1999). A role for the caveolin scaffolding domain in mediating the membrane attachment of caveolin-1. The caveolin scaffolding domain is both necessary and sufficient for membrane binding in vitro. J Biol Chem *274*, 22660-22667.

Schroeder, R.J., Ahmed, S.N., Zhu, Y., London, E., and Brown, D.A. (1998). Cholesterol and sphingolipid enhance the Triton X-100 insolubility of glycosylphosphatidylinositol-anchored proteins by promoting the formation of detergent-insoluble ordered membrane domains. J Biol Chem *273*, 1150-1157.

Sedding, D.G., and Braun-Dullaeus, R.C. (2006). Caveolin-1: dual role for proliferation of vascular smooth muscle cells. Trends Cardiovasc Med *16*, 50-55.

Shao, Y., Akmentin, W., Juan Jose Toledo-Aral, J.R., Gregorio Valdez, John B. Cabot, Brian S. Hilbush, and Simon , and Halegoua, S. (2002a). Pincher, a pinocytic chaperone for nerve growth factor/TrkA signaling endosomes. J. Cell Biol. *157*, 679-691.

Shao, Y., Akmentin, W., Toledo-Aral, J.J., Rosenbaum, J., Valdez, G., Cabot, J.B., Hilbush, B.S., and Halegoua, S. (2002b). Pincher, a pinocytic chaperone for nerve growth factor/TrkA signaling endosomes. J Cell Biol *157*, 679-691.

Sharma, D.K., Choudhury, A., Singh, R.D., Wheatley, C.L., Marks, D.L., and Pagano, R.E. (2003). Glycosphingolipids internalized via caveolar-related endocytosis rapidly merge with the clathrin pathway in early endosomes and form microdomains for recycling. J Biol Chem *278*, 7564-7572.

Shaul, P.W., and Anderson, R.G. (1998). Role of plasmalemmal caveolae in signal transduction. Am J Physiol *275*, L843-851.

Sjoblom, B., Ylanne, J., and Djinovic-Carugo, K. (2008). Novel structural insights into F-actin-binding and novel functions of calponin homology domains. Curr Opin Struct Biol *18*, 702-708.

Small, J.V., Isenberg, G., and Celis, J.E. (1978). Polarity of actin at the leading edge of cultured cells. Nature *272*, 638-639.

Smart, E.J., Graf, G.A., McNiven, M.A., Sessa, W.C., Engelman, J.A., Scherer, P.E., Okamoto, T., and Lisanti, M.P. (1999). Caveolins, liquid-ordered domains, and signal transduction. Mol Cell Biol *19*, 7289-7304.

Smith, C.A., Dho, S.E., Donaldson, J., Tepass, U., and McGlade, C.J. (2004). The cell fate determinant numb interacts with EHD/Rme-1 family proteins and has a role in endocytic recycling. Mol Biol Cell *15*, 3698-3708.

Tagawa, A., Mezzacasa, A., Hayer, A., Longatti, A., Pelkmans, L., and Helenius, A. (2005). Assembly and trafficking of caveolar domains in the cell: caveolae as stable, cargo-triggered, vesicular transporters. J Cell Biol *170*, 769-779.

Thomsen, P., Roepstorff, K., Stahlhut, M., and van Deurs, B. (2002). Caveolae are highly immobile plasma membrane microdomains, which are not involved in constitutive endocytic trafficking. Mol Biol Cell *13*, 238-250.

Torgersen, M.L., Skretting, G., van Deurs, B., and Sandvig, K. (2001). Internalization of cholera toxin by different endocytic mechanisms. J Cell Sci *114*, 3737-3747.

Tsao, S.C., Su, Y.C., Wang, S.L., and Chai, C.Y. (2007). Use of caveolin-1, thyroid transcription factor-1, and cytokeratins 7 and 20 in discriminating between primary and secondary pulmonary adenocarcinoma from breast or colonic origin. Kaohsiung J Med Sci *23*, 325-331.

Welte, M.A. (2004). Bidirectional transport along microtubules. Curr Biol *14*, R525-537.

Wood, S.A., Park, J.E., and Brown, W.J. (1991). Brefeldin A Causes a Microtubule-Mediated Fusion of the Trans-Golgi Network and Early Endosomes. Cell *67*, 591-600.

Yamamoto, M., Toya, Y., Jensen, R.A., and Ishikawa, Y. (1999). Caveolin is an inhibitor of platelet-derived growth factor receptor signaling. Exp Cell Res *247*, 380-388.

Yang, Y.S., and Strittmatter, S.M. (2007). The reticulons: a family of proteins with diverse functions. Genome Biol *8*, 234.

Zerial, M., and McBride, H. (2001). Rab proteins as membrane organizers. Nat Rev Mol Cell Biol *2*, 107-117.